TRIBHUVAN UNIVERSITY

INSTITUTE OF ENGINEERING

PULCHOWK CAMPUS

THESIS NO: 078/MSCCD/006

Application of Glacio-hydrological degree-day Model to simulate hydrological regime of Tamakoshi River Basin, Nepal

By

NABIN CHAULAGAIN

(078/MSCCD/006)

DEPARTMENT OF APPLIED SCIENCE AND CHEMICAL ENGINEERING

INSTITUTE OF ENGINEERING, TU

A THESIS

SUBMITTED TO DEPARTMENT OF APPLIED SCIENCE AND CHEMICAL ENGINEERING PARTIAL FULFILMENT OF THE REQUIREMENT FOR THE DEGREE OF MASTER OF SCIENCE IN CLIMATE CHANGE AND DEVELOPMENT

DEPARTMENT OF APPLIED SCIENCE AND CHEMICAL ENGINEERING

LALITPUR, NEPAL

DECEMBER 2023

COPYRIGHT

TRIBHUVAN UNIVERSITY

INSTITUTE OF ENGINEERING

PULCHOWK CAMPUS

DEPARTMENT OF APPLIED SCIENCE AND CHEMICAL ENGINEERING

The undersigned certify that they have read, and recommended to the Institute of Engineering for acceptance, a thesis entitled "**Application of Glacio-Hydrological Degree-day Model to Simulate Hydrological Regime of Tamakoshi River Basin, Nepal**" submitted by **Nabin Chaulagain (078MSCCD006),** in partial fulfillment of the requirements of the degree of **Master of Science (M.Sc.)** in **Climate Change and Development** Programme.

Supervisors:

……

Prof. Dr. Rijan Bhakta Kayastha
Department of Environmental Science and Engineering, School of Science
Kathmandu University

..……..

Prof. Dr. Khem Narayan Poudyal
Climate Change and Development Programme, Department of Applied Science and Chemical Engineering,IOE, Pulchowk Campus

Head of Department:

…….

Prof. Dr. Hem Raj Pant
Department of Applied Science and Chemical Engineering

MSCCD Coordinator:

……

Prof. Dr. Rinita Rajbhandari
Climate Change and Development Programme, Department of Applied Science and Chemical Engineering,IOE, Pulchowk Campus

External Examiner:

…….

Assoc. Prof. Dr. Dhiraj Pradhananga
Department of Meteorology, Tri-Chandra Multiple Campus, Tribhuvan University

Date: December 2023

ACKNOWLEDGEMENT

I am extremely thankful to my supervisors Prof. Dr. Rijan Bhakta Kayastha, Department of Environmental Science and Engineering, School of Science, Kathmandu University and Prof. Dr. Khem Narayan Poudyal, Department of Applied Science and Chemical engineering, IOE, Pulchowk Campus for their guidance, support with full encouragement and enthusiasm.

I am grateful to Prof. Dr. Rinita Rajbhandari, Coordinator, Climate Change and Development Programme, IOE, Pulchowk Campus, for her valuable suggestions, and ever-encouraging and motivating guidance.

Last but not least, I would also like to thank all of my friends, family members for encouraging and supporting me whenever I needed them.

Nabin Chaulagain

078/MSCCD/006

ABSTRACT

The glaciers and snow-covered areas has been highly influential in the hydrology of the glacierized basin. Long-term water management will become more difficult as a result of climate change, which is anticipated to alter water availability. Here we have set up Glacio-hydrological Degree day Model Version 2 (GDM V.2) as a hydrological model to simulate the discharge in Tamakoshi River basin (TRB) and quantified various runoff components. The model is first calibrated and validated for the period of 2004-2009 and 2011-2020, respectively where Nash-Sutcliffe Efficiency (NSE) is 0.77 and 0.80 for calibration and validation periods. The monsoonal rain was anticipated to influence stream flow changes the most (46.86%), followed by base flow (37.57%), snowmelt (12.17%), and ice melt (3.18%) form the year 2004-2009 and rain (46.33%), followed by base flow (38.79%), icemelt (3.27%), and snowmelt (10.77%) from 2011-2020 according to the model. Forecasts indicate a rise in discharge under SSP58.5, notably reaching 3.68 m^3/s according to EC-Earth3, in stark contrast to the declines projected under SSP24.5, such as the decrease to 0.09 m^3/s under Nor ESM2-MM, between SSP24.5 and SSP58.5, constituent contributions exhibit significant variations, shedding light on potential shifts in resource availability. During the low-flow phase from May to June, substantial icemelt and snowmelt contribute to stream runoff. Yet, increasing temperatures could diminish snowfall and glacier coverage, potentially impacting future river discharge adversely. The fluctuating peak values underscore the significant impact of varying components over different time frames, a phenomenon primarily attributed to climate change. In SSP24.5, base flow ranges from 31.78% to 32.07%, ice-melt from 8.85% to 11.83%, rainfall from 46.71% to 53.65%, and snowmelt from 5.4% to 6.8%. In SSP58.5, ice-melt sees an increase to 12.58% to 19.06%, snow melt fluctuates between 5.2% and 6.54%, while rainfall and base flow remain relatively stable. The Glacio-hydrological Degree-day Model (GDM) emerges as valuable tool for comprehending hydrological dynamics and evaluating potential climate change impacts on Himalayan river basins. The insights from this study are anticipated to raise awareness about the effects of climate change on future water flow.

Keywords: Climate change, Degree day factor, Hydrological modelling, Glacio hydrological Degree-day model, Tamakoshi River Basin

TABLE OF CONTENTS

LIST OF SYMBOL AND ABBREVIATIONS

IPCC	Intergovernmental Panel on Climate Change
SRES	Special Report on Emissions Scenarios
GDM	Glacio hydrological Degree-day Model
RCP	Representative Concentration Pathway
GHG	Greenhouse gases
GCM	Global circulation model
RCM	Regional climate model
CORDEX	Coordinated Regional Downscaling Experiment
SWAT	Soil and Water Assessment Tool
HBV	Hydrologiska Byråns Vattenbalansavdelning model
HEC-HMS	Hydrologic Engineering Center – Hydrologic Modeling System
TRB	Tamakoshi River Basin
ICIMOD	International Centre for Integrated Mountain Development
CMIP6	Coupled Model Inter comparison Phase
NASA	National Aeronautics and Space Administration
T	Temperature
P	Precipitation
H	Historical
O	Observed
S	Second
NSE	Nash Sutcliffe efficiency
m a.s.l	Mean above sea level
DHM	Department of Hydrology and Meteorology
LAT	Latitude
LONG	Longitude
ELEV	Elevation
DEM	Digital elevation model
ET	Evapotranspiration
EQM	Empirical Quantile Mapping
GAWSER	Guelph All Weather Sequential Event Runoff
ASCAT	Advanced Scatterometer
SDSM	Statistical downscaling model

WGS	World Geodetic System
UTM	Universal Transverse Mercator
ESRI	Environmental Systems Research Institute
Yr	Year
Km	Kilometer
%	Percentage
&	Ampersand

LIST OF FIGURES

LIST OF TABLES

CHAPTER ONE: INTRODUCTION

1.1 Background

Majority of experts believe that people are solely to blame in an era of accelerating global climate change. The Fourth Assessment According to the Intergovernmental Panel on Climate Change (IPCC, 2007), during the twenty-first century, there is growing conviction that some extremes will become more habituated, broad and intense. An impact on snow and glacier areas can be seen due to rise in temperature and climate change resulting in future water supply downstream. A substantial impact on human and biological systems are expected due to Changes in normal climatic circumstances, as well as catastrophic events (MOONEY, 2005). Nepal well known as south Asian water tower, however there is uncertainty to regional hydrology and difficulties in water resource management all because of climate change (Devkota & Gyawali, 2015). Water resources are particularly vulnerable to climate change variables such as precipitation and temperature. Climate change is likely to alter water supply through affecting hydrological variables such as precipitation and temperature, which affect the hydrological cycle (Mengistu et al., 2021). Storing around 75% of the world's freshwater, Glaciers are a crucial component of the climate system. Because to their proximity to human populations, alpine glaciers are indispensable in terms of utilizable water (Singh et al., 2006). Snow as well as glacier melt areas contribute notably to stream flow in snow and glacier-fed river basin systems (Khadka et al., 2014). Changing climate hold hydrological processes that alter river flow regimes and freshwater availability in catchment-scale hydrology in the Himalayan River basin (Adhikari et al., 2022). Area and glacier volume appear to be directly proportional to season intensity and inter annual variation in runoff (Juen et al., 2007). Glacier melt is expected to increase until 2050, then decrease in the sub-basins (Immerzeel et al., 2013). Regionally, discharge is forecasted to increase until 2050, then vice-versa (Lutz Arthur et al., 2016). While around 53 million people live within the 2400 km of the Himalayas, above one billion people living downstream depend on HMA water for food and energy production (Apollo, 2017). Previously in order to explore the potential impact of climate change on water supplies, various methodologies and models have been pre-owned. The effects of climate change on a river basin's hydrology as well as water resources should be simulated using well-calibrated and validated models, as well as different climate scenarios, to present a credible and robust estimate of uncertainty (Li et al., 2016). As a consequence, the employment of multifarious climate and hydrological models is required

to assess the response of hydrology to changing climate in a systematic manner, eventually estimating the future state of these water resources. Conducted a systematic review of hydrological responses to climate change and discovered that higher uncertainty was caused by hydrological models in comparison to climate models.

The most recent climate scenario is Shared Socioeconomic Pathways (SSP) as per 6th IPCC assessment report. It has a diverse set of policy options for mitigating and adapting to climate change. As a result, SSP refers to a collection of socioeconomic challenges that must be addressed in order to mitigate and adapt. As a result, SSPs are the result of a social trend of making mitigation or adaptation decisions without considering climate change (Daigneault et al., 2018). Projections from General Circulation Models (GCMs) are crucial in understanding upcoming climate changes. Nonetheless, the spatial resolution at which GCMs are conducted is frequently too coarse to obtain meaningful projections at the regional and local scales. For climate impact assessments, higher spatial resolution precipitation and temperature estimates are essential. Moreover, precipitation and temperature from GCMs have a biasness due to their coarse resolution or model parameterizations. A hydrological model is a simplified depiction of the Earth's water processes. Using hydrological models such as, HEC-HMS, SPHY Model, HBV Model, and, GDM, SWAT water availability and future consequences on stream flow regimes are also investigated. In conclusion, for modelling the complex interplay between glaciers, climate and hydrology, hydrological models provide a solid foundation. Predicting stream flow patterns under various climatic scenarios provides useful insights into the possible implications of climate change on water supply, assisting policymakers and stakeholders in developing adaptation solutions (Shea et al., 2015). Accuracy and dependability can be improved after the inclusion of remote sensing data, ground observations and meteorological inputs into these models, allowing for a thorough examination of glacier melt processes and their downstream implications. Nonetheless, it's critical to acknowledge the uncertainties that come with glacio-hydrological modeling, especially when estimating future stream flows under changing climate circumstances. It is critical to address these uncertainties by ongoing refining of model parameters, to maintain the trustworthiness of model outcomes, incorporation of advanced climate forecasts, and validation against observed data. Furthermore, the socioeconomic aspects of water resource management must not be disregarded, as changes in stream flow patterns can

have far-reaching consequences for agriculture, energy production, ecosystems, and livelihood (IPCC), 2019).

To address these challenges, the Glacio-hydrological Degree-day Model (GDM), Version 2.0, has been developed as a gridded and distributed Glacio hydrological model (Kayastha et al., 2020). This model can simulate different runoff components contributing to total discharge, including snowmelt, glacier ice melt, rainfall, and base flow, on a daily basis. GDM is particularly effective in Himalayan catchments characterized by data scarcity due to challenging terrain and limited weather stations. It can operate with minimal data and a limited number of model parameters (Khadka et al., 2020).

1.2 Statement of Problem

In glacierized basin hydrology, Glaciers and snow-covered areas, a vital role is played. In coming day's snow cover and water availability is projected to alter creating difficulties in long-term water management climate change (Khadka et al., 2014). Modelling enrich to generate the future scenarios assisting in offing adaptation and mitigations.

Approximately by 25% Nepal's total glacier area has recede during the last three decades (ICIMOD, 2014). Not only that, precipitation that contributes to snowfall will diminish, causing river flow to increase even further. A high impact can be found on rivers in mountainous catchment due to climate change. It is critical to estimate and foresee snow runoff and ice runoff as snow melt process is sophisticated, complex, and temperature dependent. The latest climate projection of the CMIP6 model was presented in Climate Change Assessment Report 6, which gives better projection and higher sensitivity than the previous one. In this River Basin, no studies on SSP scenarios have been conducted to understand impact of climate change on recent scenarios applying this GDM model.

Frequently Glacierized areas suffer from an insufficient data on multifarious hydro-meteorological factors such as temperature, precipitation, and glacier mass balance. The quality and quantity of accessible data have a significant impact on the accuracy and dependability of model findings. For proper glacier modeling one must understands the complicated dynamics of ice movement, melting, calving, and buildup. Elements such as temperature, topography, and glacier geometry are impacted by these process, creating hurdles in model representation. The combination between glacier melt and downstream water supply can have serious socioeconomic consequences. It is important to incorporate

socioeconomic aspects into the model and examine the potential repercussions of changing glacier dynamics on local people.

To date on the timing and evolution of glaciers, as well as the associated changes in runoff minimum studies have been carried out. Some studies have been conducted referring A comprehensive study of the response of glacierized basins to climate change in the Himalayas, owing to inaccessible terrain, a lack of observed climatic data, and the fact that glacier response is not systematic across the Himalayas (Khadka et al., 2020).

1.3 Objectives

1.3.1 General Objective

- The primary objective of this research is to apply a Glacio-hydrological Degree-day Model (GDM) to simulate stream flow in the Tamakoshi basin.

1.3.2 Specific Objective

- To set up the GDM in the Tamakoshi River Basin and analyze the hydrological regime of the river.
- Evaluating the model's performance in simulating stream flow under various climatic and glacier change scenarios.

1.4 Scope of work

The primary thrust of this investigation lies in unearthing, assessing, and consolidating the reservoir of insights embedded in prior research articles concerning climate change in Nepal. Within this expansive domain, the investigative lens zeroes in on the intricate realm of water resources, with a particular emphasis on the Tamakoshi Basin. This study's core endeavor revolves around dissecting the intricate web of climate change's ripple effects on the hydrology of the Tamakoshi basin. This analytical journey draws its sustenance from an exhaustive evaluation of hydro-meteorological and spatial data culled from the upstream catchments that encompass the Tamakoshi basin's watershed.

A key juncture of the study entails the deliberate selection of an apt modeling framework for the watershed, and herein, the GDM takes center stage. This choice is rooted in an all-encompassing appraisal, encompassing a spectrum of Climate projection General Circulation Models (GCMs). Furthermore, the research meticulously singles out the most pertinent projections within the CMIP6-GCMs suite, precisely tailored to align with the

geographic scope of the study, thereby setting the stage for insightful glimpses into the future. Armed with this chosen model, the research aspiration extends to refining the precision of assessing and forecasting hydrological responses.

This intricate endeavor encompasses the simulation of hydrological trajectories within the confines of two distinct scenarios, borne from CMIP6-GCMs climate projections. By seamlessly weaving forthcoming climatic data from CMIP6 into the framework of the GDM model, this study endeavors to unveil the latent repercussions that lay ahead.

1.5 Limitation of the study

Various characteristics, parameters and coefficients for specific basins are important in this investigation, which may not be feasible so a standard value may be used. Since, majority of the glacier is located in Tibet, the required meteorological and hydrological observation data set may not be accessible and must be projected using Nepali reference station data. Insufficient data in the Tamakoshi river basin is the most significant restriction of our investigation. Long-term hydro-meteorological data from a wide number of sites would have contributed to a more trustworthy conclusion. Station spatial distribution was likewise inadequate throughout the chosen area. The absence of recent years of data series may limit the ability to incorporate recent changes brought about by climate change in hydrology.

The research heavily relies on a land use and cover map for modeling glacier ice melt in a basin. The absence of projected changes in land use and cover is a significant limitation, impacting the accuracy of future glacier ice melt assessments. The study lacks validation for individual discharge components (rain, snowmelt, icemelt, baseflow) and an Isotope test is proposed to scrutinize whether simulated contributions align with observed data. Besides this the dependency on the accuracy and quality of the GCM data used for future projection may also limit the result of this study.

CHAPTER: TWO LITERATURE REVIEW

2.1 Climate change

Primarily driven by industrialization's march forward, the concentration of greenhouse gases and CO_2 within the Earth's atmosphere has witnessed a momentous surge since 1950. The undeniable impact of human activities on the Earth's climate system is evident in various ways, including rising temperatures, changes in precipitation patterns, more frequent and severe extreme weather events, and the rapid melting of snow and glaciers in recent decades (D. Khadka & Pathak, 2016). In response to these challenges, there has been a concerted global effort to reduce carbon emissions, with the goal of limiting the increase in global temperatures to less than 1.5°C by the end of the century (Lima & Gupta, 2013). This movement has led to a significant increase in research focused on regional-scale climate projections and a growing interest in understanding how these changes will impact water resources and hydropower.

As a result, there has been a noticeable surge in research and exploration in these areas. Scientists and researchers are actively studying how climate change will affect the availability and distribution of water resources, as well as the feasibility and sustainability of hydropower projects in a changing climate. This increased attention reflects the urgency of addressing climate change and its potential impacts on essential aspects of our environment and energy systems.

The anticipated consequences of climate change on the environment encompass a range of significant impacts, including rising temperatures, increased instances of flooding, diminished water resources, health risks, and a decline in biodiversity (NASA). The average global temperature has increased by approximately 0.8 degrees Celsius since 1880, with a substantial portion of this rise occurring after 1975 at a rate of 0.15-0.2 degrees Celsius per decade. Notably, the three-decade period from 1983 to 2012 is recognized as the warmest in the last 1400 years (Knutti et al., 2013).

In-depth analysis of long-term climate changes in the Mediterranean region and southern Europe has underscored a notable increase in heat waves and the consequences of droughts in recent years (Carnicer et al., 2011). As the climate continues to warm, the likelihood of flooding becomes more pronounced. While a limited number of global studies have begun to scrutinize changes in flood occurrence, none have comprehensively addressed this issue within the context of a hotter climatic system (Hirabayashi et al., 2013). These findings

highlight the urgency of understanding and mitigating the environmental and societal impacts of climate change.

2.2 Climate change in Nepal

Nepal is currently grappling with the consequences of climate change, which include rising temperatures, shifts in precipitation patterns, and the gradual disappearance of glaciers. These changes have significant implications for Nepal's water resources, agricultural productivity, and ecological balance.

Climate-related shifts, including alterations in temperature, precipitation patterns, and the frequency of extreme weather events, have the potential to cause significant impacts on various sectors, such as water availability, disaster risk reduction, agriculture, industry, and recreational activities. A substantial portion of Nepal's population is at risk due to these climate change impacts, including threats like reduced agricultural yields, food insecurity, increased pressure on water resources, forest and biodiversity degradation, and compromised infrastructure. Nepal saw an annual temperature increase of 0.056°C, with the most pronounced warming evident at elevated altitudes in the high mountains and the Himalayas by the latest report of DHM, Government of Nepal. It is anticipated that the severity of these consequences will worsen unless effective adaptive measures are put in place (Mengistu et al., 2021).

2.3 Climate model

Climatic models are critical tools for developing views of probable future climatic situations. They work by modelling the complex interplay of the global climate system and its underlying processes, particularly as it relates to the effects of human-caused climate change. General Circulation Models (GCMs) are a sort of major climate model with a somewhat coarse spatial resolution. While these models are unable to capture fine-scale features, they do combine regional shifts to provide insight into larger global transitions (Bergdtrom Sten et al., 2001). The General Circulation Model (GCM) is a complex mathematical and numerical design. It applies fundamental ideas such as like as the Navier-Stokes equations and thermodynamics to simulate the complicated dynamics of the Earth's atmosphere and oceans. GCMs provide a very comprehensive model of atmospheric phenomena and are well suited for long-term temporal scales and large spatial coverage.

According to the 6th IPCC assessment report, the most recent climate scenario is Shared Socioeconomic Pathways (SSP). It has a diverse set of policy options for mitigating and adapting to climate change. As a result, SSP refers to a collection of socioeconomic challenges that must be addressed in order to mitigate and adapt. As a result, SSPs are the result of a social trend of making mitigation or adaptation decisions without considering climate change (Daigneault et al., 2018). Projections from General Circulation Models (GCMs) are critical in understanding future climate changes. However, the spatial resolution at which GCMs are conducted is frequently too coarse to obtain meaningful projections at the regional and local scales. Higher spatial resolution precipitation and temperature estimates are necessary for climate impact assessments. Furthermore, precipitation and temperature from GCMs have a bias due to their coarse resolution or model parameterizations. Many methodologies and models have been used in the past to explore the potential impact of climate change on water supplies On a river basin's hydrology, the effects of climate change and water resources should be simulated applying well-calibrated and validated models, as well as various climate scenarios, to deliver a credible and robust estimate of uncertainty (Li et al., 2016). Correspondingly, the employment of different climate and hydrological models is important to assess the response of hydrology to fluctuating climate in a systematic manner, in due course estimating the upcoming state of these water resources. Conducted a systematic review of hydrological responses to climate change and discovered that uncertainty caused by hydrological models was greater than uncertainty created by climate models.

However**,** Applying using them for climate projection requires accepting various assumptions and dealing with inherent uncertainties. These uncertainties stem from a multiple variety of sources, including the amount of greenhouse gas emissions, the model's intricate architecture, the initial conditions set at the model's boundaries, methodologies for downscaling from larger scales to local levels, and techniques for correcting inherent biases (Ghimire et al., 2019). Given the possibility of biases introduced by these models when compared to observable data, the pursuit of enhanced GCM output involves the use of optimal procedures and methodologies. A prudent plan entails using various GCMs to analyze and contrast their findings, the most credible model for future forecasts is identified. Furthermore, a variety of bias-corrected climate projection data, such as CMIP6 data, is now available, which contributes to improving projection accuracy (Mishra et al., 2020).

In summary, climate models are a critical entryway to understanding what lies ahead for our planet's climate. The complicated interplay of numerous components, the need to balance assumptions with uncertainties, and the pursuit of greater accuracy all highlight the dynamic and varied nature of climate modeling. We get ever deeper insights into the complicated dance of Earth's climate system as knowledge develops and these models evolve.

2.4 Hydrological Models

A hydrological model is a mathematical depiction of the processes that influence water transport and distribution within a certain area or watershed. These models are used to represent the hydrological cycle's behavior, which includes processes such as precipitation, evaporation, infiltration, runoff, and stream flow. Hydrological models assist researchers, water resource managers, and policymakers in understanding how water moves through the terrain, forecasting changes in water availability, and making informed water management decisions. Hydrological model are classified into lumped model, semi-distributed and distributed model.

2.4.1 Lumped model

Lumped rainfall and runoff models are simpler, more extensively utilized, and operate in a single homogeneous unit. In addition, they need less input data than distributed and semi-distributed models. The model does not represent the physical properties of hydrologic processes.

2.4.2 Semi distributed model

The semi-distributed model is also known as the simplified distributed model. Because parameters vary over space, divide the basin into multiple sub basins. Semi-distributed model types include HEC-HMS, TOPMODEL, SWAT, and others. Unlike TOPMODEL, which use a probability distribution of input parameters over the basin, HEC-HMS employs an equation for surface and subsurface flow. In terms of structure, semi-distributed models have the advantage of being more physically based than lumped models (Cunderlik et al., 2003).

2.4.3 Distributed model

Distributed hydrologic models can be utilized for the most accurate simulation of precipitation-runoff processes. Because they are entirely spatially variable at a given

resolution, the parameters of these models are substantially more complex than those of semi-distributed models. Distributed models include the Guelph All Weather Sequential Event Runoff (GAWSER), MIKE11/SHE, and CASC2D (Cunderlik et al., 2003). GDM (Glacio Hydrological Degree Day Model) is both dispersed and gridded. Flood forecasting, flood control, land use and climate change effect assessments, pollution control, and other applications all make extensive use of distributed models. Input data for these models include topography, vegetation, land use and land cover, rainfall, evaporation, soil properties, vegetation, and so on (Ghimire et al., 2019).

2.5 Modelling Approaches

In contemporary practice, the realm of glacier melt modeling encompasses two predominant techniques: the energy balance approach and the temperature index model. These methods are widely employed across various global regions to compute discharge in river basins with glacier coverage. The energy balance method breaks down melt as a residual term in the surface energy balance equation, carefully taking into account the total energy flows in the atmosphere and along the edge of the glacier. (Reid & Brock, 2010). Conversely, the temperature index model hinges on empirical relationships between air temperatures and the pace at which melting occurs (Braithwaite, 1995; Hock, 2003). While the energy balance approach excels in capturing comprehensive melt quantities (Hock, 1999, 2003) its utility faces limitations for Himalayan glaciers located in remote terrains where data availability remains a challenge (Kayastha et al., 2000).

The fundamental objective of hydrological models is to replicate the intricate flow patterns emerging under a diverse array of circumstances or scenarios, effectively encapsulating the essential mechanisms governing the hydrological cycle. This intricate emulation process closely mirrors the inherent natural processes (Ghimire et al., 2019). To achieve this, these models engage in the simulation of basin runoff, employing variables such as precipitation, air temperature, relative humidity, alongside additional inputs involving the basin's topography, land cover, and soil attributes. The scope of applications for hydrological models is expansive, covering domains like water resource planning and development, in-depth flood analysis, precise quantification of water quality and quantity, and the comprehensive assessment of climate change impacts.

Several hydrological models have been developed in recent years such as HBV model (Bergström, 1992; Meteorological, 2015), SWAT model (Arnold et al., 1998), JAMS

J2000 model (Krause, 2002), SPHY model (Terink et al., 2015), GDM model (R. B. Kayastha & Kayastha, 2019) and many other to estimate water balance and components contributions through model parameterization (Budhathoki et al., 2023).

2.5.1 Hydrologiska Byrns avdeling for Vattenbalans (HBV) Model

It is a conceptual model that incorporates various physical processes and basin characteristics. This model relies on temperature and precipitation data as input to assess and simulate stream flow (Vormoor et al., 2018). It offers a comprehensive assessment of basin responses, encompassing factors such as precipitation, climate, land use, water balance, flow patterns, the impacts of climate change, flood characteristics, as well as the intricate interplay between soil and water, and sediment yields (Adhikari et al., 2022).

As highlighted by (Seibert & Vis, 2012; van Tiel et al., 2020), the HBV-light version includes functionalities for handling precipitation in snowy conditions, soil moisture dynamics, chemical reactions, and routing mechanisms that account for the presence of lakes and glaciers (Seibert, 2005). Importantly, this model provides continuous discharge simulations at different elevations, considering both glacierized and non-glacierized zones, and can be applied to specific sites within the basin area.

2.5.2 Spatial Processes in Hydrology (SPHY) Model

Spatial Processes in Hydrology (SPHY) v3 model as outlined by (Terink et al., 2015), is a spatially distributed water balance model characterized as a "leaky-bucket" type. It is specifically designed for conducting large-scale studies on cryosphere-hydrological interactions and incorporates various hydrological components, encompassing (a) the transformation of rainfall into runoff, (b) processes related to the cryosphere, (c) evapotranspiration, and (d) soil hydrological mechanisms. An important feature of SPHY is its adaptability to various spatial scales, making it suitable for analyses at sub-basin, basin, and regional levels.

2.5.3 Jena Adaptable Modelling System (JAMS J2000) Model

Designed with an open modeling philosophy in mind, the J2000 system provides a versatile set of capabilities for preprocessing input data. These functionalities encompass tasks such as correcting precipitation data, regionalizing climate data obtained from specific locations, and computing potential evapotranspiration, as outlined in the works of (Krause, 2002; Krause & Kralisch, 2005). The J2000 system integrates distinctive

features, including a modular design that accommodates self-contained program modules for runoff simulation. Operating within an object-oriented framework, these modules receive data, produce results, and seamlessly interchange with others, enhancing adaptability for future improvements without necessitating a full model reconstruction. (Krause & Kralisch, 2005).

2.5.4 Soil Water Assessment Tool (SWAT) Model

SWAT functions as both an operational and conceptual model, operating on a daily time scale. Its primary goal during development was to project the impact of management practices on water, sediment, and agricultural chemical yields within extensive, ungauged basins. To achieve this objective, the model (a) eliminates the necessity for calibration, which is often impractical in ungauged basins; (b) relies on readily available input data that is applicable to vast geographical areas; (c) demonstrates computational efficiency suitable for large basins within reasonable timeframes; and (d) maintains continuous operation, enabling the simulation of outcomes resulting from management changes over extended periods (Arnold et al., 1998).

2.5.5 Hydrologic Modeling System (HEC HMS) Model

The Hydrologic Modeling System (HEC-HMS) is a meticulously designed tool crafted to emulate the intricate processes of precipitation-runoff within dendritic drainage basins. Its inherent versatility allows for its application in diverse geographical regions, addressing a wide range of challenges. These applications span from managing water resources in extensive river basins and forecasting floods to dealing with smaller-scale concerns like runoff in urban or natural watersheds. The hydrographs generated by HEC-HMS serve practical purposes, either independently or in conjunction with other software tools. They support various studies related to the availability of water resources, urban drainage, flow prediction, the potential impacts of future urban development, the design of reservoir spillways, flood damage reduction, floodplain regulation, and systems operation.

2.5.6 Glacio-hydrological Degree-day Model (GDM)

The GDM Version 2.0 is a distributed and gridded Glacio-hydrological model that simulates daily river discharge and calculates the contribution of snow melt, ice melt, rain, and base flow to river discharge, according to (Kayastha et al., 2020; Kayastha & Kayastha, 2019). The melt module in GDM uses a temperature index model to perform

the basic approach for modelling glacio-hydrological events. GDM is calibrated based on essential calibration parameters such as positive degree-day factors, snow and rain runoff coefficients, and recession coefficients Positive degree-day factors and critical temperature values are obtained from previous research in central Himalayan catchments (Kayastha et al., 2005; Khadka et al., 2015).

The utilization of OGEM and GDM in projecting stream flow alterations within the Urumqi river head watershed in the Tianshan Mountain region, China, demonstrated the GDM's greater sensitivity to shifts in air temperature than changes in glacier extent (Yang et al., 2022).

2.6 Glacio-Hydrological Degree-Day Model (GDM)

GDM is helpful for Himalayan catchments where data is scarce due to difficult terrain and an insufficient number of meteorological stations, GDM can function with low data and minimum model parameters. The parameters of the melt module, such as the degree-day factors for snow and ice melt, are derived from field observations conducted in the Nepal Himalayas. (Kayastha et al., 2000). Degree-day factor for ice melt under a debris layer is assumed to be around half of the clean ice melt based on the field observation on Khumbu and Lirung Glaciers in Nepal Himalayas. Many researcher has been working on the field of glaciology modeling with this model (Table 2.1).

In order to estimate potential evapotranspiration using the Thornthwaite equation, monthly sunlight hours must be added to these components. The possible solar hours estimates are based on previous research (Niroula et al., 2015). The model separately estimates melt for snow, clean ice and ice under debris based on the degree-day approach (Braithwaite & Olesen, 1989; Kayastha et al., 2005). The equations used in the model can be referred from (Kayastha et al., 2020).

Table 0.1 Summary of application of Glacio Hydrological Degree-Day model for different study with their major findings.

Study Area	Objectives	Major Findings	References.
Marsyangdi and Trisuli River basin, Nepal	GDM useful for Himalayan River basin	The model has the potential to be a useful tool for researching the dynamics of hydrological systems and the consequences	(Kayastha & Kayastha, 2019)

		of climate change on Himalayan river basins.	
Koshi River basin, Nepal	Future projection of cryospheric and hydrologic regimes in Koshi River basin, Central Himalaya, using coupled glacier dynamics and glacio-hydrological models	Most sub-basins experience a shift in peak flow from August to July. This study's linked modeling technique can greatly enhance our understanding of glacio-hydrological dynamics in the Himalayan region.	(Khadka et al., 2020)
Marsyangdi, Trisuli and Tamor River Basin, Nepal	Comparative study of hydrology and icemelt in three Nepal river basins using the GDM and observation from the ASCAT	ASCAT GM detects glacier melting at higher elevations than GDM but lacks the precision to capture complex ablation zone processes, as evident from modeling and satellite data.	(Kayastha et al., 2020)
Karakoram, Pakistan	Multi-model assessment of glacio-hydrological changes in central Karakoram, Pakistan	The restructured melt and baseflow modules in GDM have fundamentally enriched our Perception of glacio-hydrological dynamics in the Catchment.	(Hassan et al., 2021)
Tianshan Mountain, China	Projection of Stream flow Changes Under CMIP6 Scenarios in the Urumqi River Head Watershed	It was discovered that a 2°C increase in the monthly average temperature might result in a 37.7% increase in the basin's total discharge. Furthermore, the GDM was more sensitive to changes in air temperature than changes in glacier size.	(Yang et al., 2022)

2.7 Terms Used in the Model

Table 2.2 shows the parameters and features used in GDM.

Table 0.2 Parameters and features used in Glacio-Hydrological Degree Day Model

Grid:	Number of grids in which the study basin is divided
Reference Station Elevation:	Base station elevation for temperature (T) and precipitation (P) in m a.s.l.
Lower/Higher Elevation:	Lower elevation (LE) is usually the elevation from where glacier starts.
Higher elevation (HE):	Elevation from where the degree day factors need to be changed. These LE and HE are used to assign different degree-day factors for the basin.
Debris-covered glacier area:	Area of the basin covered by debris-covered glacier (km2) (If the basin does not has debris-covered glacier ice, then the debris-covered glacier area at each zone = 0)
Clean glacier area	Area of the basin covered by a clean glacier (km^2)
k:	Degree-day factor (mm/°C/d); ks and kb refer to degree-day factors for snow and ice melt, respectively. These values may differ according to the elevation of the basin, which is denoted by LE and HE for lower elevation and higher elevation, respectively. • k [LE] represents the degree-day factors for the elevation zones that starts from the lower elevation to zone below higher elevation defined by the user.

	• k [HE] represents the degree-day factors for the elevation zones that start from the higher elevation defined by the user.
Cr and Cs:	Cr and Cs: Runoff coefficient expressing losses as a ratio of the measured precipitation to the measured runoff, where Cr and Cs refer to rain coefficient and snowmelt runoff coefficients, respectively. The program accepts different values of Cr and Cs for different months.
Critical Temperature:	Whether the measured precipitation is rain or snow at that temperature is determine by Critical temperature (°C)
Temperature lapse rate:	Temperature lapse rate (°C/100 m) can be obtained from the temperature stations available at different elevations within the basin or from nearby stations that can represent the climatic condition of the basin. The program accepts different temperature lapse rate values for different zones.
x and y:	x and y are the constants used to calculate the recession coefficient (k)
Model Accuracy:	The model accuracy can be assessed thorough two accuracy criteria: Nash – Sutcliffe Coefficient (Nash and Sutcliffe 1970).

	$$NSE = 1 - \frac{\sum_{i=1}^{n}(Q_i - Q_i')^2}{\sum_{i=1}^{n}(Q_i - \bar{Q})^2}$$ Where n : Number of days Q_i: Daily measured discharge Q'_i: Simulated measured discharge $\bar{Q}$: Average discharge of the given year in m^3/sec. ii. Volume Difference: $$VD(\%) = \frac{V_R - V_R'}{V_R} \times 100$$ where V_R: Measured runoff volume V'_R: Simulated runoff volume in m^3.

CHAPTER THREE: DATA COLLECTION AND METHODOLOGY

3.1 Study Area

The Tamakoshi River is a trans-boundary Himalayan river basin and one of the major tributaries of the Koshi river basin system, located in eastern Nepal on the central Himalayas' southern slope. The basin is situated geographically on Dolakha and Ramechhap districts of Nepal form the country's political boundary. The basin is 2937.509 square kilometers having perimeter of 365.23 kilometers at the Busti gauging station, with 1,444.57 square kilometers on Chinese territory. Tamakoshi river basin is located at latitudes 27°20' N to 28°20' N and longitudes 85°40' E to 86°40' E, with heights ranging from 857 m a.s.l to 7323 m a.s.l nearby Mt. Cho Yu. Over 39% of the catchment (1163 km^2) is over 5000 m a.s.l. This basin is predicted to have 85 glaciers covering a total area of 84.4 square kilometers in 2010 (ICIMOD, 2014). This basin's climate is subtropical at low levels and tundra at higher elevations (Karki et al., 2016). From June to September, The summer monsoon, has huge influence on the climate of the study area. The climate also differs from lower to higher altitude, in the high Himalayas. In summer and winter the basin's average temperature is 28 degrees Celsius and 7 degrees Celsius respectively, the minimum temperature in the study region falls below freezing. During the winter, in the higher Himalayas. Yearly rainfall in the study area is roughly 1900 mm, with 80% falling during the summer monsoon (Aryal et al., 2019). The study area including the hydro-meteorological stations and the stream flow is shown in Figure 3.1.

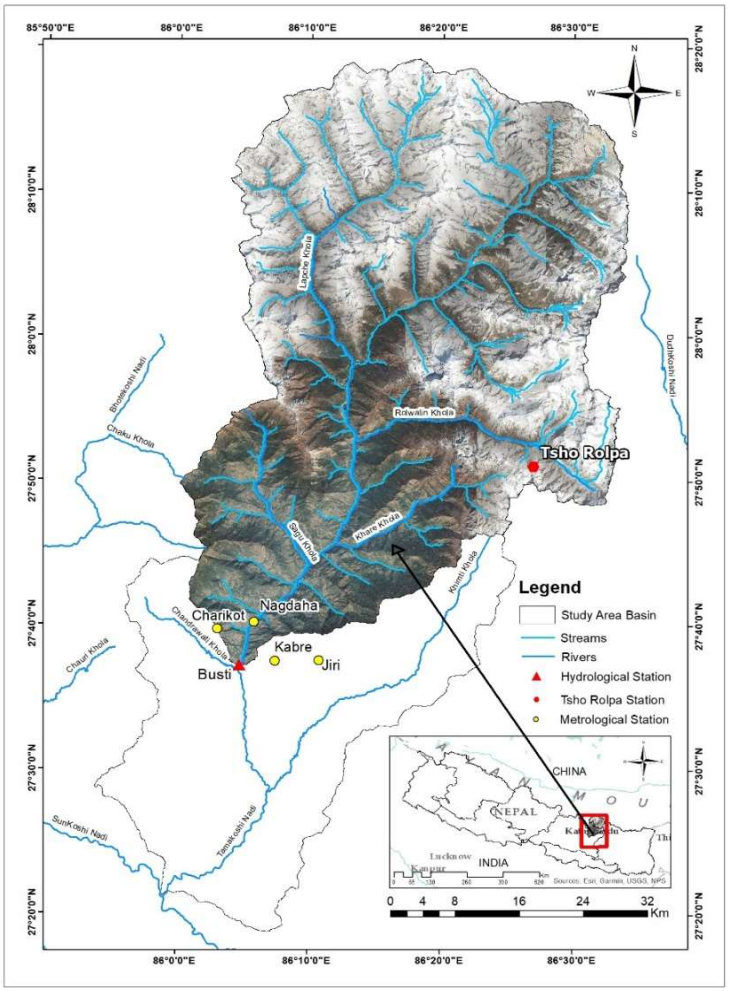

Figure 0.1 Study Area (Tamakoshi River basin) showing the stream flow along with hydro-meteorological stations used for the study within the basin.

3.2 Data collection

3.2.1 Hydrology and Meteorology

Hydro-Meteorological data were collected from the Department of Hydrology and Meteorology (DHM), Government of Nepal. Overall, Four meteorological and one hydrological stations were used in this study, the daily observed precipitation data were collected form Nagdaha (1101), Charikot (1102), Jiri (1103) and Kabre (1124) whereas daily observed temperature data was only for station Jiri (1103). The hydrological data i.e. the daily discharge data was collected from Busti station (647). Data is used for the calibration and validation of the Hydrologic model. The meteorological data are precipitation, maximum temperature, and minimum temperature data. The daily observed

Meteorological data from DHM range from the year 2004 to 2020. There are many flaws and gaps in the data provided by DHM. Therefore for better analysis and interpretation the baseline data from DHM was taken for 32 years. For the purpose of model calibration and validation, we have employed weather data from 2004 to 2009 for calibration and from 2011 to 2020 for validation, on total the calibration period is taken as six years and validation is taken ten years. The stations used in the study area with its location and elevation are shown in the Table 3.1.

Table 0.1 Description of the hydrological and metrological station of the study area with its station id, location, elevation and frequency of the data availability.

Hydro-Meteorological Stations						
Station ID	Location	Type	Latitude (DD)	Longitude (DD)	Elevation (m)	Frequency
1101	Nagdaha	Precipitation	86.104	27.676	909	Daily
1102	Charikot	Climatology	86.05	27.667	1940	Daily
1103	Jiri	Agrometeorology	86.232	27.630	1877	Daily
1124	Kabre	Agrometeorology	86.142	27.639	1755	Daily
647	Busti	Discharge	86.086	27.635	849	Daily

3.2.2 Topography/Spatial Data

Grid elevation data in GDM is calculated using the Advanced Space borne Thermal Emission and Reflection Radiometer (ASTER), Global Digital Elevation Model (GDEM) v3, with a resolution of 30 meters, available from the United States Geological Survey (USGS) (M. Khadka et al., 2020). Using Arc GIS, downloaded data was projected to WGS 1984 UTM Zone 45N and then clipped to create the DEM of the research region. The clipped DEM is then used to fill the pits and sinks in the dataset, followed by the development of flow direction and flow accumulation maps and further used in the GIS Software and GIS processing were performed to obtain basin characteristics as flow path length, slope of basin, basin relief and drainage density. The elevation ranges from 857 m a.s.l to 7323 m a.s.l nearby Mt. Cho Yu. Over 39% of the catchment (1163 km^2) is over 5000 m a.s.l. Elevation wise DEM of the study is shown in Figure 3.2.

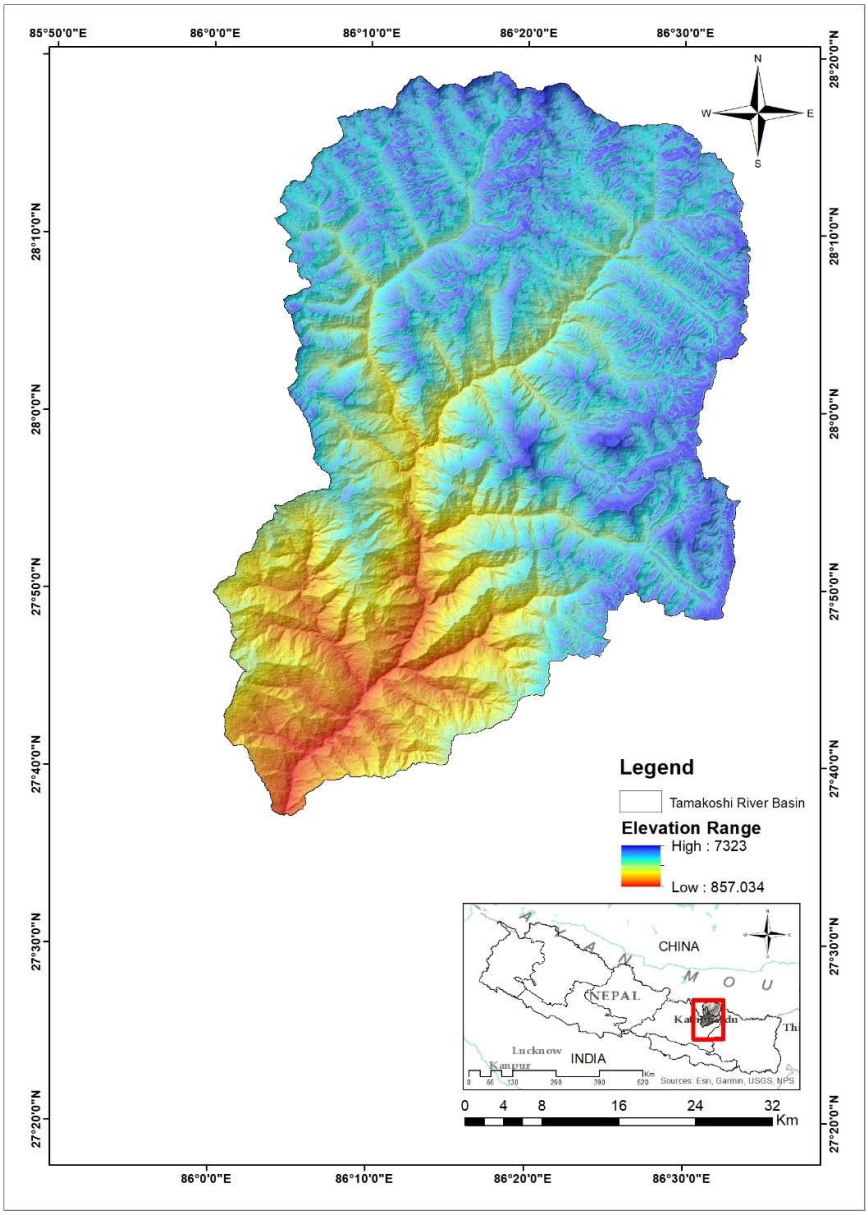

Figure 0.2 Digital Elevation Model of the study area (elevation ranges from 857 m a.s.l to 7323 m a.s.l)

3.2.3 Land use map

Since the study area encompasses high mountains, crop fields, forests, and glaciers so land use and land cover data will be needed and the model required eight classes of land cover. Global land use/land cover data with a 10 m resolution from Sentinel-2 was acquired from ESRI. The inventory of clean and debris-covered ice glaciers was sourced from the (RGI Consortium, 2017). The dataset, titled "Randolph Glacier Inventory - A Dataset of Global

Glacier Outlines, Version 6," is available in the form of a shape file. It was published by the National Snow and Ice Data Center in Boulder, Colorado, USA, and can be accessed at https://doi.org/10.7265/4m1f-gd79. The land use data was extracted with a resolution of 10 meters from ESRI and introduced into GIS software to be classified for clean and debris-covered glacier information (Karra & Kontigs, 2021). The land use pattern of the study area has been given in Figure 3.3. The components included in the Tamakoshi basin are around forest (20%), crops (0.35%), grassland (32%), bare lands (33%), wet lands (0.65%), settlements (2%), debris covered glaciers (3%) and clean glaciers (9%). The classification of the land use and land cover is as shown in Figure 3.4. The reclassification of the land use and land cover using the LULC is in Figure 3.5. In the study area, eight different land use types are preserved. The majority of the area is covered by grass land and bare land, followed by forest. Water, crops, and built-up areas cover a smaller area than other types. The land use changes has great impact on discharge of the river and evapotranspiration (Wegehenkel, 2002).

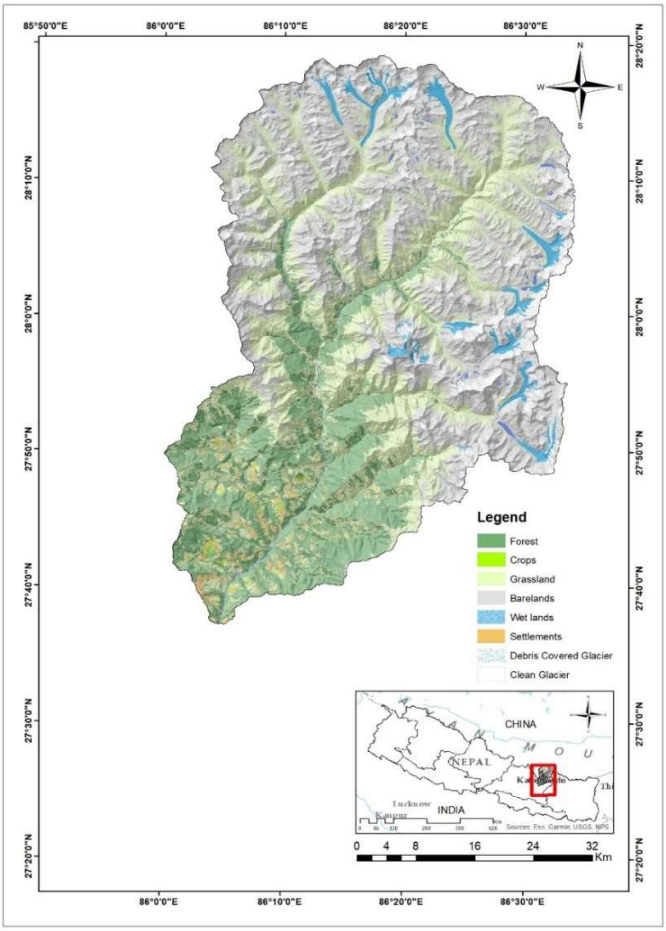

Figure 0.3 Land use map of the study area showing the eight different classification of land use.

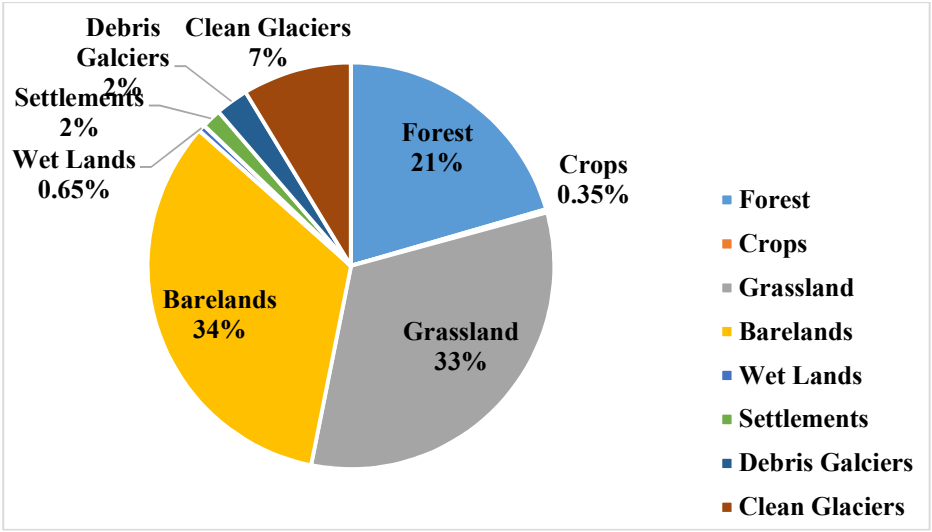

Figure 0.4 Pie Chart showing Land Cover classification of the study area in Percentage.

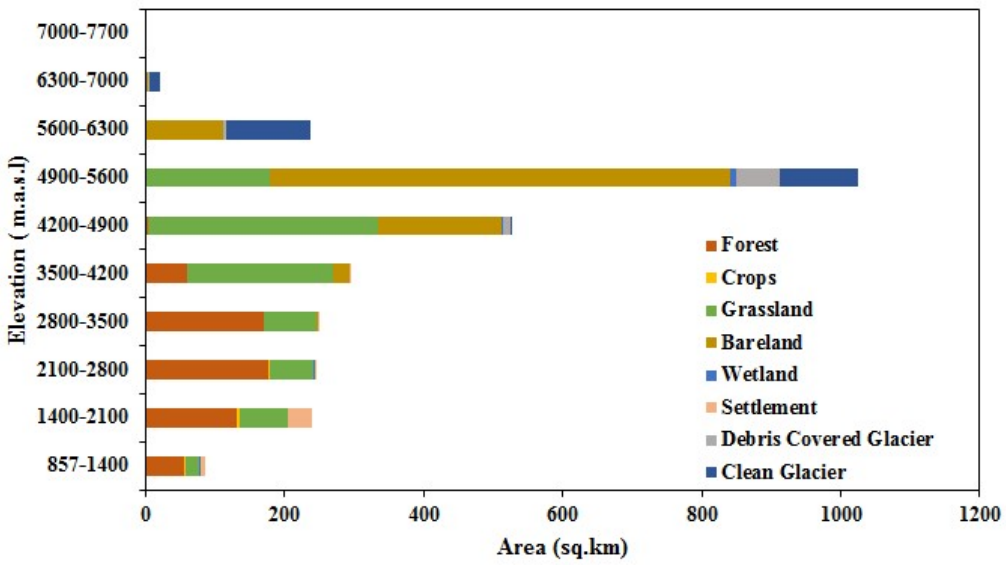

Figure 0.5 Area-altitude distribution of debris covered and clean ice along with other land use types in Tamakoshi river basin based on Aster GDEM V3 of 30 m resolution, ESRI Sentinel-2 and Randolph Glacier Inventory (2017).

3.3 Bias-Corrected Future Climate data

The role of Projections originating from General Circulation Models (GCMs) is pivotal in unraveling the contours of forthcoming climate shifts. However, the spatial resolution at which GCMs function often falls short of delivering reliable projections at the regional and local levels. In order to effectively gauge the consequences of climate change, higher spatial resolution is imperative for precipitation and temperature projections. Moreover, the precipitation and temperature outputs of GCMs harbor biases due to their coarse resolution and underlying model parameterizations. Consequently, in the pursuit of evaluating the impact of climate change on sectors such as water resources and agriculture, the process of bias correction becomes a requisite. To achieve this, both statistical and dynamical methodologies are employed to refine and rectify biases in climate change projections emerging from GCMs (Mishra et al., 2020).

Upon realms such as agriculture, water resources, infrastructure, and the livelihoods of millions across South Asia to unleash substantial challenges the impending specter of climate change is poised. In response, we have carefully cultivated a comprehensive dataset that encapsulates daily bias-corrected records of crucial variables including precipitation, maximum and minimum temperatures. Boasting a spatial resolution of 0.25°

this dataset encompasses an expansive expanse that includes nations such as India, Pakistan, Bangladesh, Nepal, Bhutan, and Sri Lanka. . The intricate construction of this bias-corrected dataset depend on the adept application of Empirical Quantile Mapping (EQM) techniques. 18 river basins nested within the larger Indian sub-continent, the scope of this dataset extends to encompass, while simultaneously casting its gaze into the horizon, and this dataset unfolds as a chronicle of historical records spanning 1951 to 2014, venturing into future projections from 2015 to 2100 across four distinct scenarios (SSP12.6, SSP24.5, SSP37.0, and SSP58.5). This compilation is rooted in the outputs of 13 General Circulation Models (GCMs) sourced from the Coupled Model Inter comparison Project-6. The meticulous validation process of this bias-corrected dataset entails a rigorous examination against observed data encompassing both average and extreme precipitation, along with maximum and minimum temperatures.

For bias correction, statistical transformations are employed to discover a function that links the model's output to a fresh distribution, aligning it with the distribution seen in the actual observations. Typically, this transformation can be expressed mathematically (Piani et al., 2010) (Figure 3.6).

$$x^{o}_{m} = f(x_m) \qquad (1)$$

Where x^{o}_{m} is the bias-corrected model output. If the statistical distribution of x_m and x_0 are known, the transformation can be written as:

$$x^{o}_{m} = F^{-1}_{0}\,(F_m\,(x_m)) \qquad (2)$$

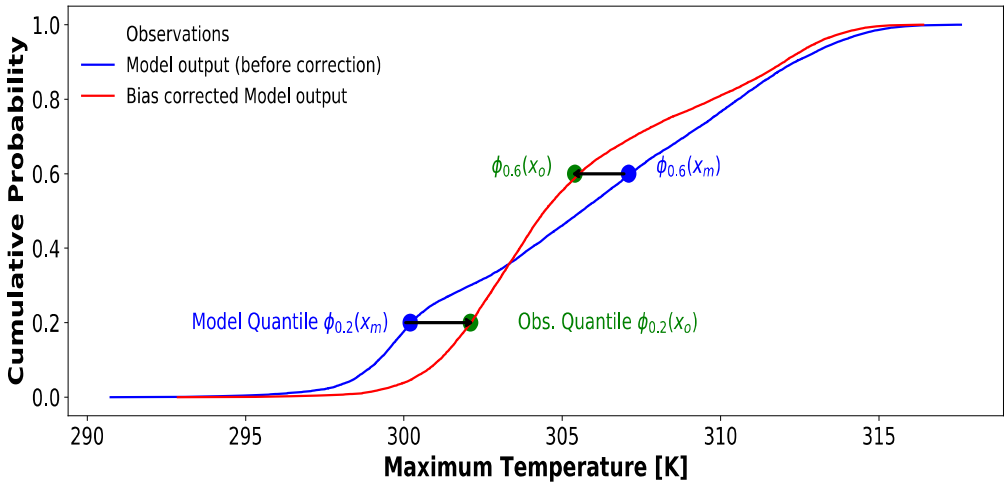

Figure 0.6 Illustration of Empirical Quantile Mapping of model output (x_m) (obtained from CMIP6 archive) and observed daily maximum temperature (x_o) over a representative grid-point chosen randomly from the Indian Subcontinent. While at 20th percentile ($\phi_{0.2}$), (x_m) is lower than (x_o) for the same quantile, (x_m) exhibits higher bias than xo at 60th percentile ($\phi_{0.6}$) (Mishra et al., 2020).

Bias-corrected projections hailing from 13 CMIP6-GCMs. Various Global Climate Models (GCMs) with spatial and daily temporal resolution from the CMIP6 dataset have been utilized as input climate data for the Global Hydrological Model (GDM). This is done to simulate forthcoming hydrological conditions, considering the SSP24.5 and SSP58.5 climate scenarios, spanning the time period from 2023 to 2050. Three GCM with high resolution namely EC-Earth 3, MPI-ESM-2-HR and NorESM2-MM data were used for the future scenario simulation out of thirteen GCMs given.

3.4 Methodological Framework of the Study

Daily extrapolated temperature and precipitation from the reference station to each grid are used to force the model for the discharge simulation. The threshold temperature (T_T) determines whether the precipitation is in the form of snow or rain in each grid in the respective time step as:

$$Precipitation = \begin{cases} rain, & if \quad T \geq T_T \\ Snow, & if \quad T < T_T \end{cases}$$

Where, T is extrapolated daily air temperature for grids and T_T is threshold temperature, both in °C. In each grid, daily ice melt from debris free and debris-covered ice and snow Melt from glacierized and glacier free areas is calculated as:

$$M = \begin{cases} Kd \text{ or } Ks \text{ or } Kb \times T & \text{if, } T > 0 \\ 0 & \text{if, } T \leq 0 \end{cases}$$

here, M is the ice or snow melt in mm day^{-1} in each grid, T is daily air temperature in °C, K_d, K_s, and K_b are the degree-day factors for debris-covered ice, snow and clean glacier ice in mm $°C^{-1}$ day^{-1}. The model takes an account for the multilayer melting of the snow above clean ice and debris-covered ice. Baseflow is calculated using a baseflow simulation approach as in SWAT. Two aquifer system: shallow and deep aquifer system concept is applied to simulate the base flow in glacier and snow melt dominated basin (Li et al., 2016; Luo et al., 2012). The advantage of two reservoir system over single reservoir system is that it releases the discharge in recession period and assures the level of discharge much more similar to observed discharge during the recession period. Figure 3.7 shows the overall framework that were carried out to analyze and evaluate the Impacts of climate change on the study area using GDM V.2.

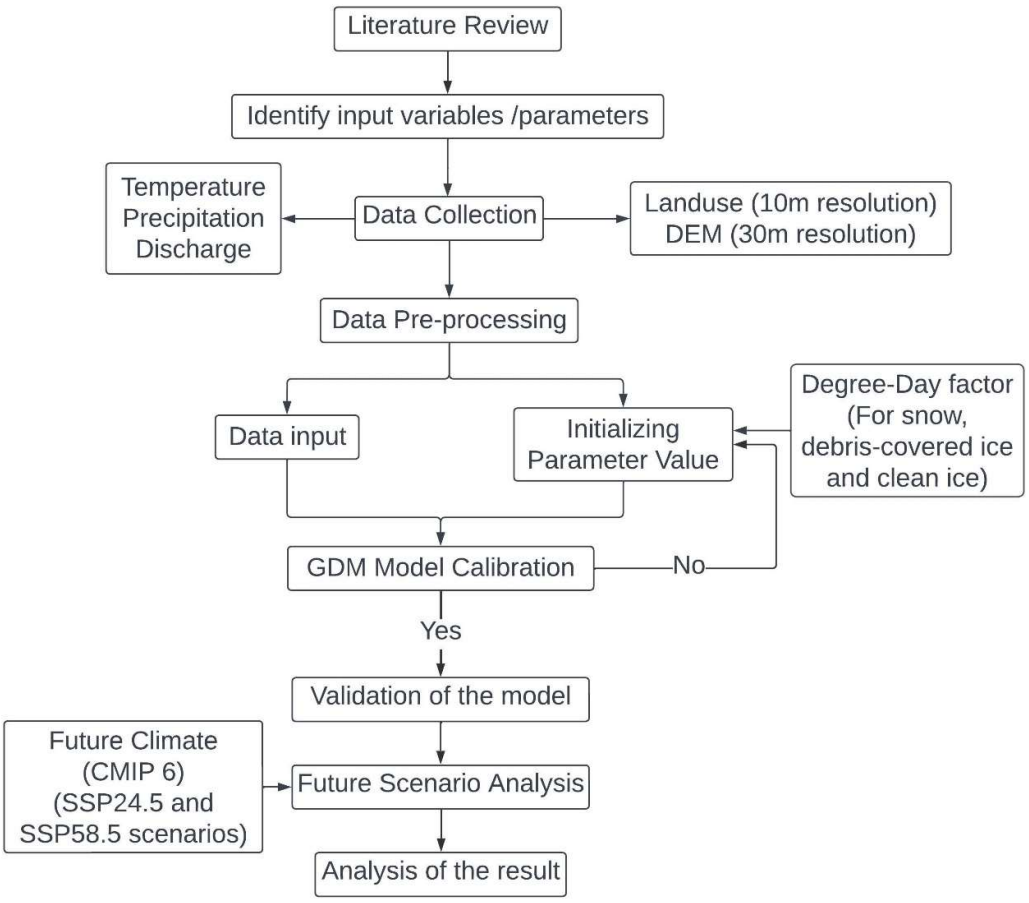

Figure 0.7 General framework of the overall study.

3.5 Filling missing data

For a hydrological model to perform, missing data must be filled in. The department of Hydrology and Meteorology provided the temperature and precipitation data used in this study. There are numerous methods for estimating missing data. Arithmetic mean method, Normal ratio method, Inverse Distance Weighted method, precipitation gradient method are few of them. The IDW (Inverse Distance Weighted) was used to fill the missing rainfall data.

The IDW method is based on the proximity of neighboring stations (or SSs) to the target station (TS). This method used distance between TSs and SSs as a weighted factor by calculating as follows:

$$W_i = \frac{d_i^{-n}}{\sum_{i=1}^{m} d_i^{-n}}$$

Where di refers to the distance between TS and SS, and m is the total number of SSs being used. The value of power "n" usually ranges from 1 to 6.

Nevertheless, the frequent used value of n is 2 (Wuthiwongyothin et al., 2021) which is also applied in this study as the distance increases, the IDW weight decreases. The value of power n is directly proportional to the distance between the stations and the less weight any one station gives to a reading assigned to a neighboring station.

At the Jiri stations, and Charikot station, the Tamakoshi Basin temperature data were accumulated. Some of the data are missing, in each station. Between 1990 and 2020 Data on temperatures were collected. There are multifarious techniques to interpolate the missing temperature data but this case uses the temperature lapse rate method. The temperature lapse rate method, in high altitude regions, is important technique for estimating missing temperature data. This method is appropriate where there is zero station and the data is extremely rare (Zhang et al., 2018). In the water sheds of the glacier and snow cover, the snow model technique uses the lapse rate method between observed and predicted stream flows the efficiency was shown to be improved by the GDM.

The basic definition of lapse rate is a temperature decrease with increasing altitude. The station-to-station lapse was obtained to identify the missing data. Stations Jiri, Charikot and Tsho Rolpa are located at elevations of 1877 m, 1940 m, and 3200 m, respectively. The lower elevation station data was used for interpolating other stations data. The basic equation used for estimating temperature data is given by:

$$L_r = \frac{T_2 - T_1}{E_2 - E_1}$$

Where,

T_1 and T_2 are mean temperature of Stations;

E_1 and E_2 are elevation of stations;

L_r = lapse rate of considered stations;

The missing temperature data were obtained using the following equation after knowing the station's lapse rate.

$T_2 = T_1 + L_r * T_1$

Where,

T_1 = known temperature data of station

T_2 = Missing temperature data of station

The missing temperature data for all stations in this study were estimated using the above two lapse rate equations.

Daily minimum and maximum temperature data and observed precipitation and observed discharge for the calibration and validation period is shown below (Figure 3.8, 3.9 and 3.10)

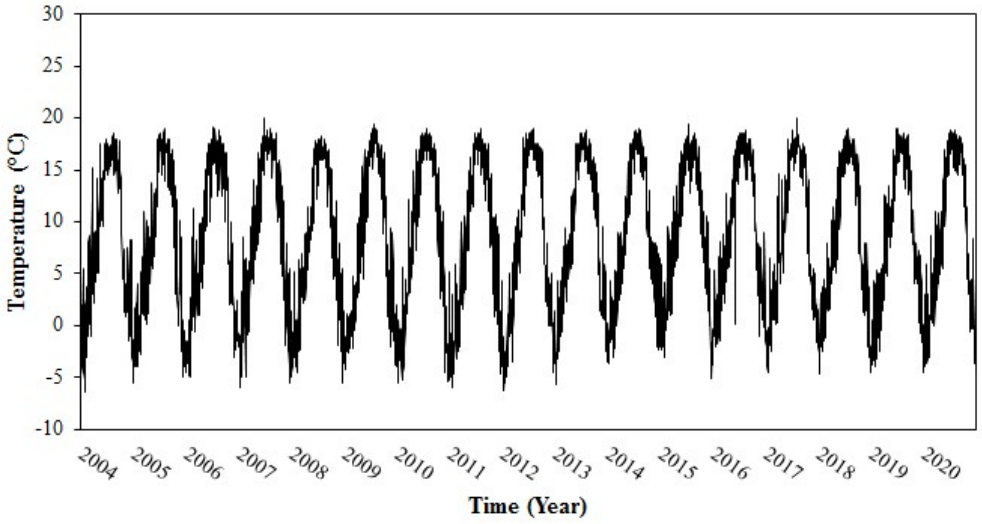

Figure 0.8 Daily minimum temperature distribution between 2004-2020 at the base station at Tamakoshi River basin

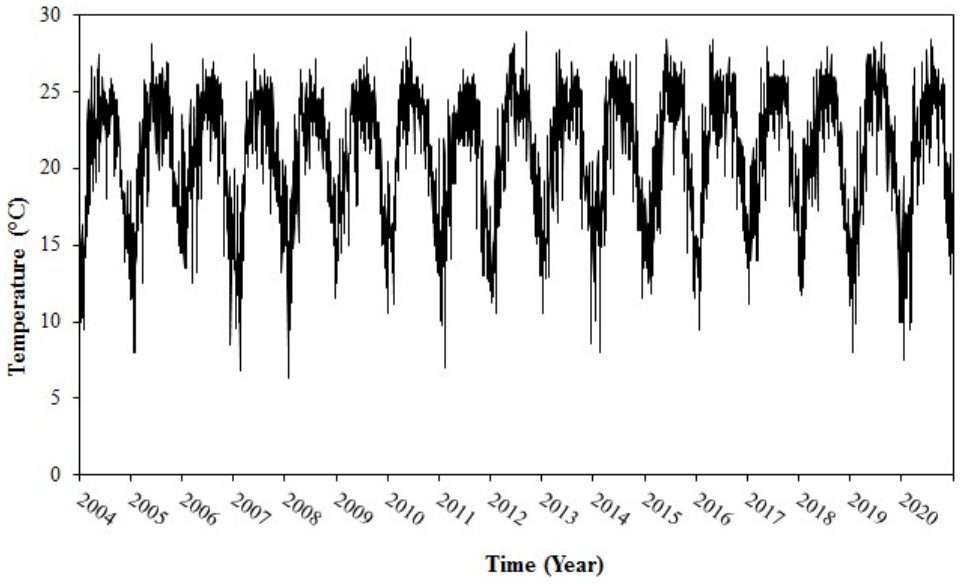

Figure 0.9 Daily maximum temperature distribution between 2004-2020 at the base station at Tamakoshi River basin

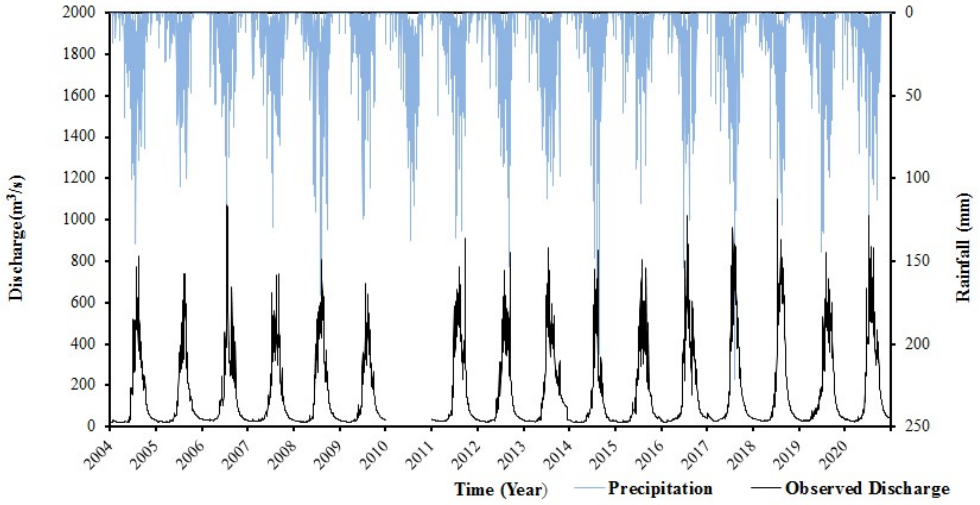

Figure 0.10 Observed average precipitation vs observed discharge at outlet of basin for the study period (2004-2020) on Tamakoshi River basin

CHAPTER FOUR: RESULTS AND DISCUSSIONS

4.1 Model Calibration and Validation

The physical-based method was used to obtain a comprehensive understanding of the basin's hydrological regime. For the hydrological simulations in the basins, GDM was calibrated. The model is calibrated using a variety of positive degree-day factors as well as a set of degree-day factors, for each month is chosen that falls within the extend of the approximated degree-day factors on various glaciers in the Nepal Himalayas. Additionally the model is calibrated with the help of ice and snow coefficients. Table 4.1 provides a list of all the calibrated variables and coefficients utilized in the investigations using GDM. The model is setup for Busti river basin station (ID 647) including the support of observed day-to-day discharge from the station and simulated discharge from the model the calibration for the year 2004-2009 and validation from the year 2011-2020 was done.

Table 0.1 Calibration parameters used in GDM and their respective values in Tamakoshi river basin

Parameters		**Unit**	**Value**
Critical temperatures for Snow/rain		°C	2
Temperature Lapse Rate (TLR)		°C 100 m^{-1}	0.58
Land constant	Land cover type 1- Forest	-	0.3-0.6
	Land cover type 2- Crops	-	0.5-0.7
	Land cover type 3- Grass land	-	0.5-0.6
	Land cover type 4- Bare Land	-	0.3-0.6
	Land cover type 5- Wet land	-	0.95
	Land cover type 6-Settlements	-	0.95
	Land cover type 7- Debris Covered Glacier	-	1
	Land cover type 8- Clean Glacier	-	1
Degree-day factor	Snow melt (k_s)	mm °C^{-1} day^{-1}	8 to 9.5
	Ice melt (clean-ice glacier) (k_b)	mm °C^{-1} day^{-1}	8 to 10.5
	Ice melt (debris-covered glacier) (k_d)	mm °C^{-1} day^{-1}	3
Recession coefficient for surface runoff (k_x)		-	0.8
Time delay for geological formation (shallow aquifer) ($\Delta_{gw,sh}$)		days	10
Recession constant (shallow aquifer) ($\alpha_{gw,sh}$)		-	0.5
Time delay (deep aquifer) ($\Delta_{gw,dp}$)		days	250
Recession constant (deep aquifer) ($\alpha_{gw,dp}$)		-	0.5
Seepage constant (deep water) (β_{dp})		-	0.8

Figure 4.1 illustrates the comparison between daily simulated discharge and observed discharge hydrograph for the Tamakoshi river basin during both calibration and validation periods. The model successfully captures both high and low observed discharge, with a minor overestimation observed in the pre-monsoon or low-flow period. This overestimation is linked to the model's representation of precipitation distribution, where the transfer from lower to higher elevations might not precisely reflect the significant variations in precipitation levels in mountainous environments, particularly in the complex topography of the high Himalayan region within the basin (Immerzeel et al., 2015). Despite these challenges, the model achieves commendable performance, as indicated by favorable Nash-Sutcliffe Efficiency (NSE) and R-squared (R^2) values, and maintains a volume difference within 10%, even with limited input data.

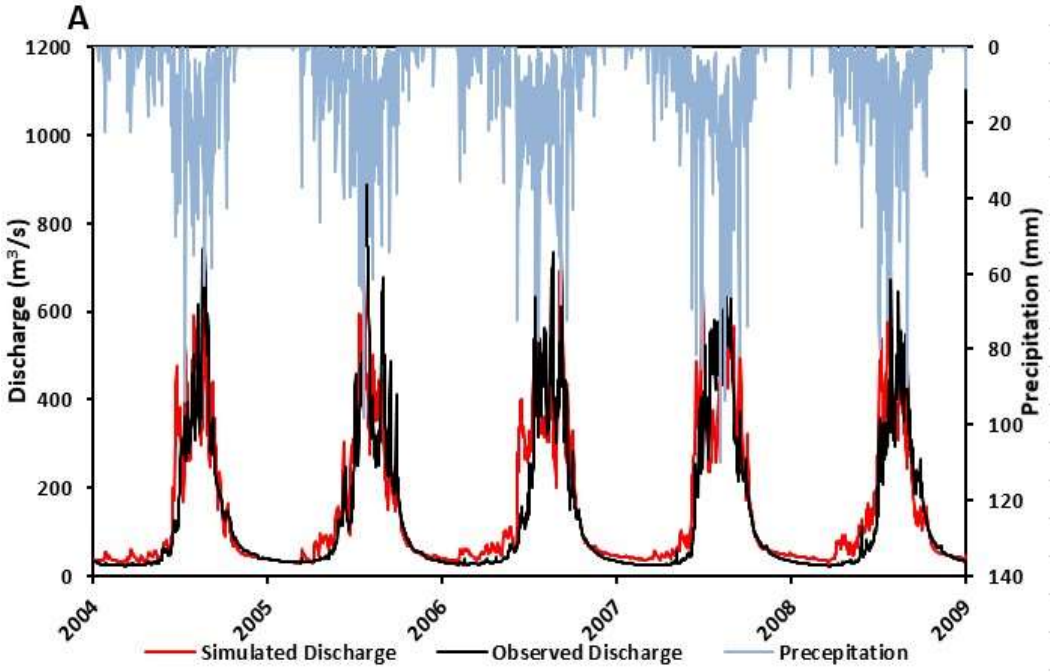

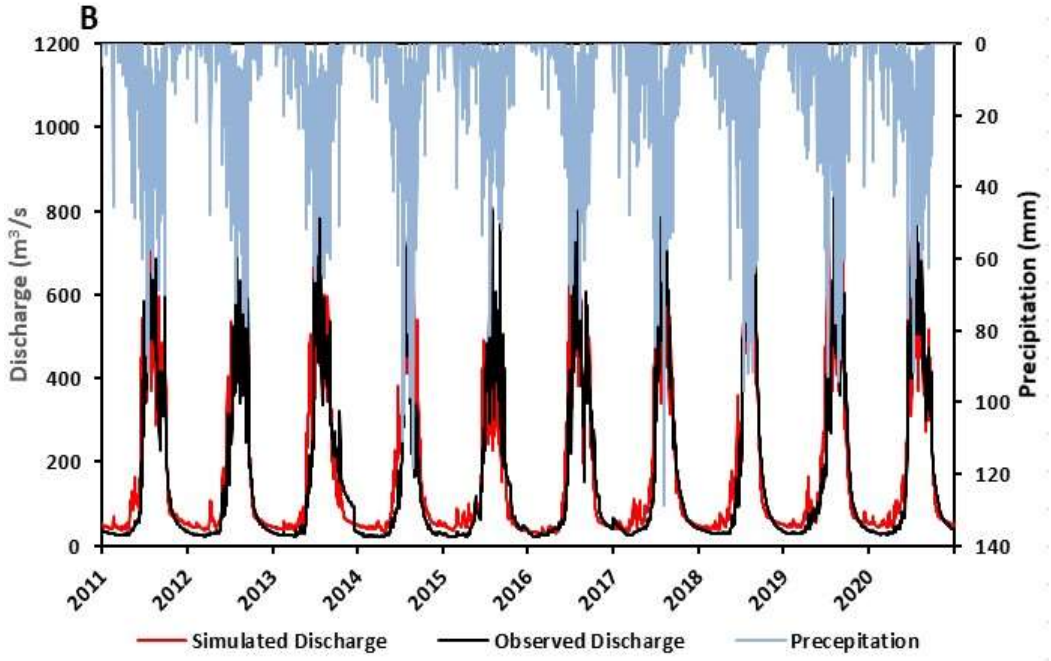
B
Discharge (m³/s
Precipitation (mm)
1200
1000
800
600
400
200
0
0
20
40
60
80
100
120
140
2011
2012
2013
2014
2015
2016
2017
2018
2019
2020
Simulated Discharge
Observed Discharge
Precepitation

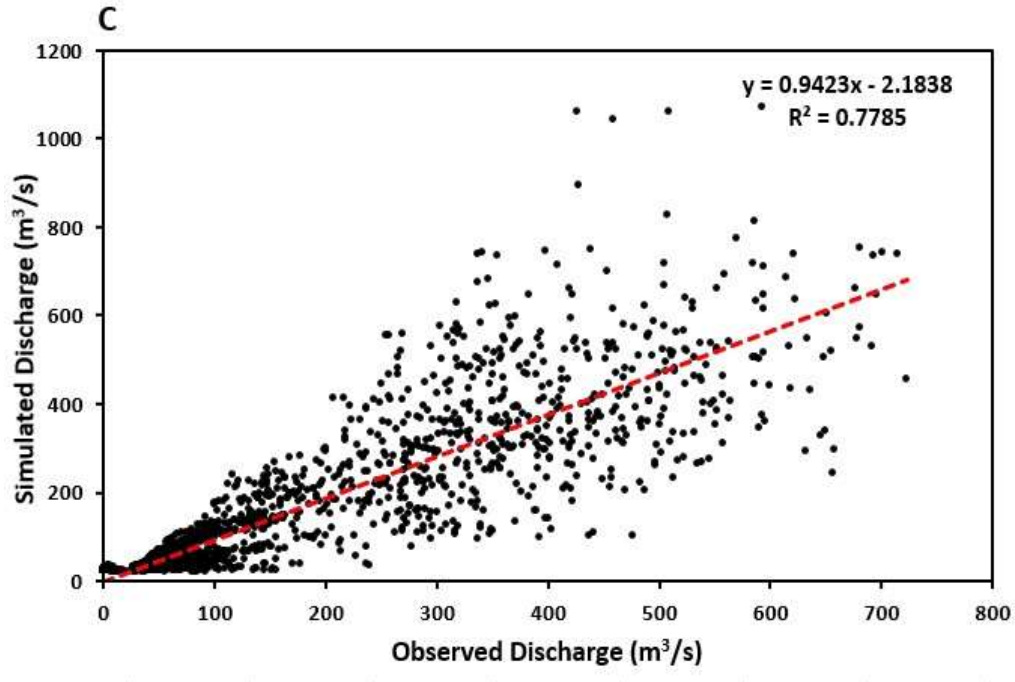
C
y = 0.9423x - 2.1838
R² = 0.7785
Simulated Discharge (m³/s)
Observed Discharge (m³/s)
1200
1000
800
600
400
200
0
0
100
200
300
400
500
600
700
800

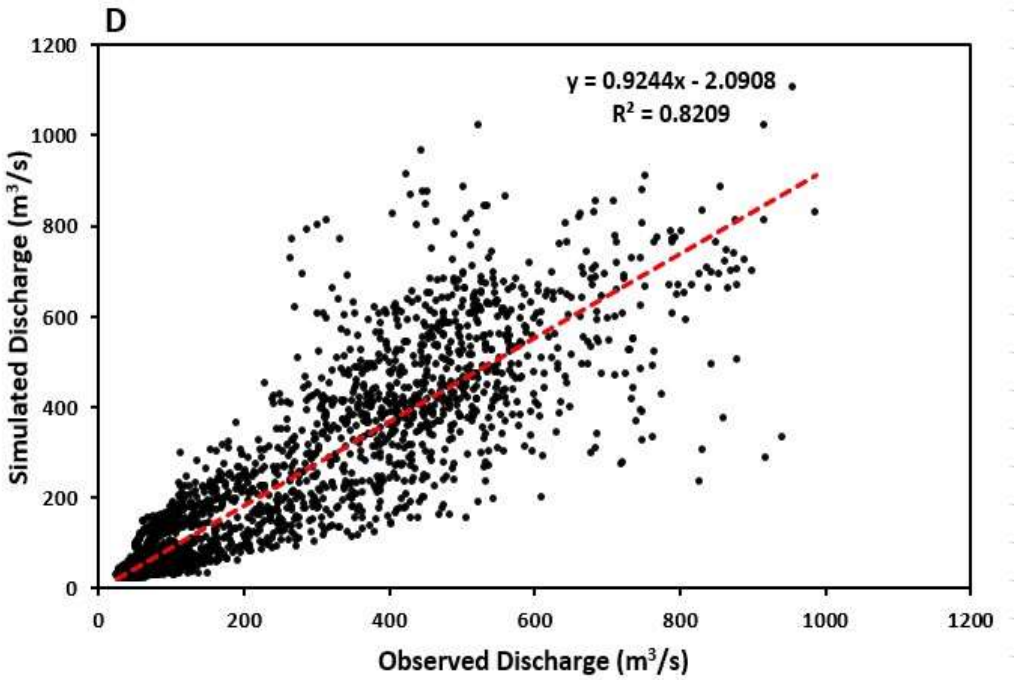

Figure 0.1 (A) Precipitation distribution and observed vs Simulated discharge for calibration period (2004-2009) ,(B) Precipitation distribution and observed vs Simulated discharge for validation period (2011-2020), (C) Scatter plots show the fit between the observed and simulated values for the calibration period (2004-2009), (D) Scatter plots show the fit between the observed and simulated values for the validation periods (2011-2020).

The best performing parameter for the basin is used to assess the model's performance. The calibration and validation (Figure 4.1 A and B) Nash-Sutcliffe Efficiency (NSE) values are 0.77 and 0.80, whereas the volume difference is 7.8% and 9.5% simultaneously and the R^2 values for calibration is 0.77 and for validation is 0.82. Hence , During the basin's calibration and validation periods ,the model's performance is very good (Da Silva et al., 2015).

4.2 Contribution of Rain, Baseflow, Snowmelt and Icemelt

The model gives the contribution of different components like Icemelt, Baseflow, Rain runoff and snowmelt that are the components of the discharge. Figure 4.2 shows the average annual monthly contributions of the discharge components for the calibration and validation period of total average annual monthly discharge. Here, snowmelt contributes 12.17% of the total annual discharge, ice melt contributes 3.18% (from clean ice and ice

under debris), rain contributes 46.86%, and base flow contributes 37.57% during the calibration period (2004-2009). Likewise, snowmelt contributes 10.77% of the total annual discharge, icemelt contributes 3.27% (from clean ice and ice under debris), rain contributes 46.33%, and base flow contributes 38.79% during the Validation period (2011-2020). Our study shows that the rain dominates the contribution in monsoon period which is followed by base flow contribution and the base flow contribution is throughout the whole year. By (Khanal et al., 2021) in Narayani river basin by SPHY model the contribution of rain runoff is 63%-65%, snow melt 9%-12% , ice melt is 3%-4% , and base flow is 21%. This research intently matches the contribution of snow melt and ice melt, besides the contribution of rain and baseflow is varied this may be due to the area coverage of the basin i.e. the Narayani basin is about 37 times bigger than our study area river basin. Hence the runoff contributions by different component is varied.

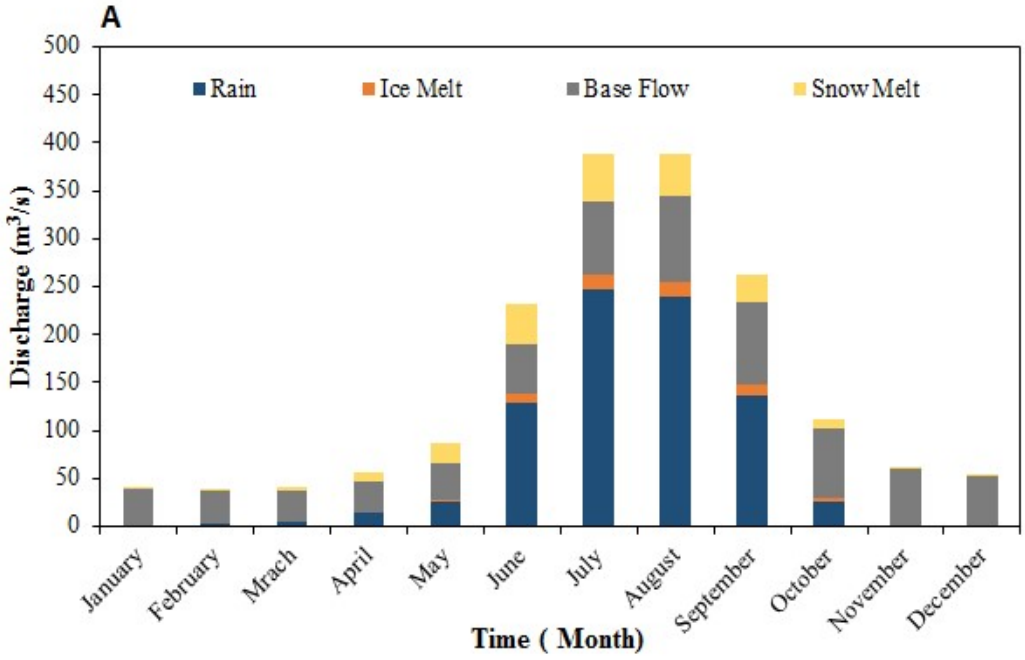

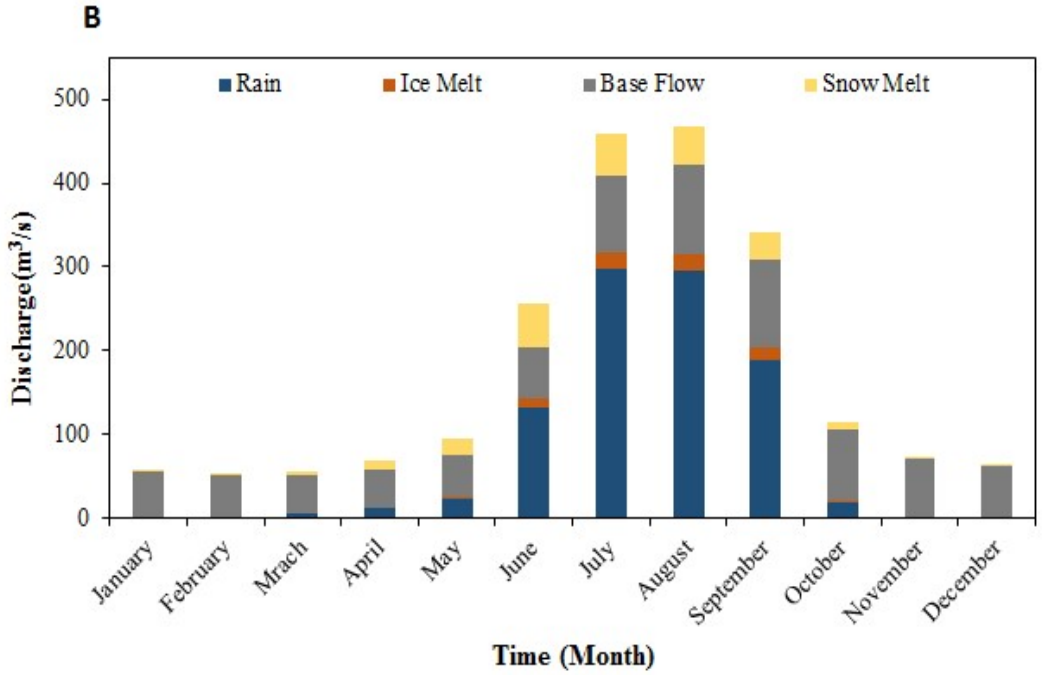

Figure 0.2 (A) Average monthly contribution of baseflow, rain, snowmelt, and icemelt for the calibration period (2004-2009) (B) Average monthly contribution of baseflow, rain, snowmelt, and icemelt for the calibration period (2011-2020).

In Figure 4.3 and 4.4, the monthly variations in the percentage contribution of icemelt and snowmelt are depicted. Significant contributions from icemelt and snowmelt to stream runoff are observed during the low-flow period between May to June. In both calibration and validation period, snowmelt and icemelt has significant contribution. In long run we can assume that the deficit of snow and ice in the basin may decrease the contribution in the flow resulting the decrement of discharge in Tamakoshi river basin. The potential consequences of rising temperatures, including reduced snowfall and glacier coverage, could have adverse effects on future river discharge.

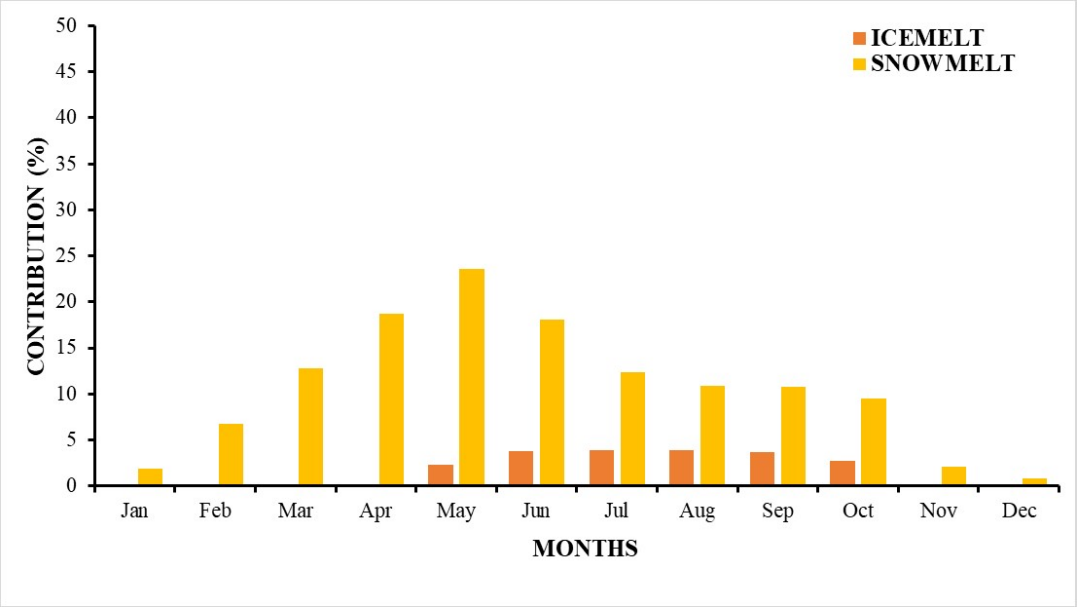

Figure 0.3 Average monthly percentage contribution graph of Snowmelt and Icemelt for calibration period (2004-2009)

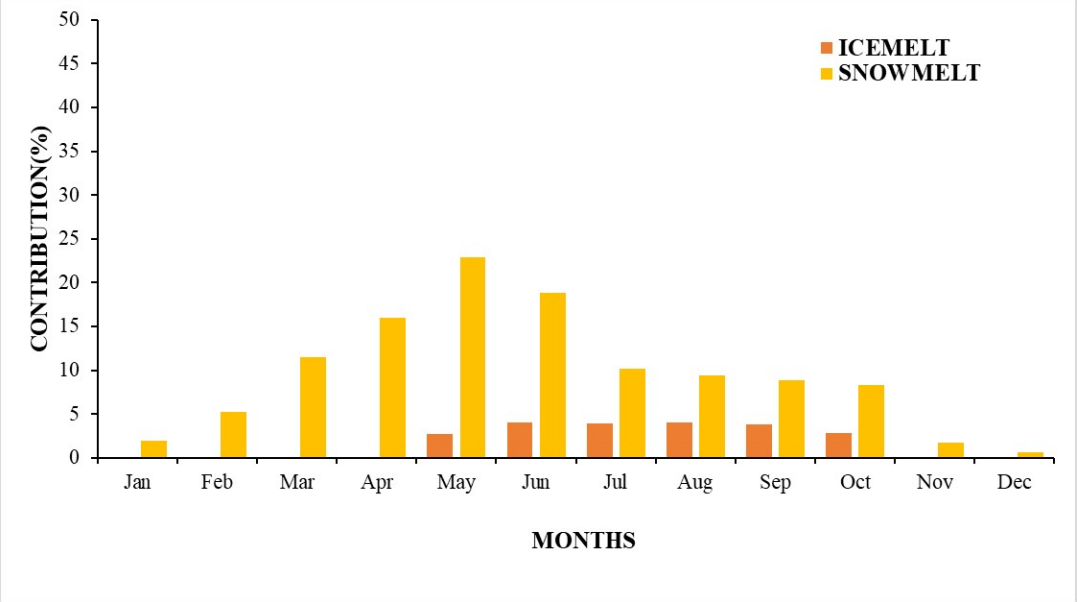

Figure 0.4 Average monthly percentage contribution graph of Snowmelt and Icemelt for validation period (2011-2020)

4.3 Future Precipitation and Temperature Trend

The projected data were bias corrected within the basin using bias correction method. The analysis of the future climate is conducted for a 27-year period, from 2021 to 2050. Since future land cover change has not been taken into account in our analysis, we have not

extended our projection into the far future (beyond 2050). Our model is descriptive in nature and may model various glacial melt trends in the future, as well as other physical aspects of the basin We have incorporated yearly precipitation and average temperature data from the three Global Circulation Models (GCM) into the GDM in order to anticipate future discharge. It is anticipated that both temperature and precipitation will rise in the next years. The entire year will see an increase in temperature, with springtime forecasting the highest increase and summertime being the lowest in Tamakoshi river basin (Khadka et al., 2014).

The different trend of future precipitation and temperature form the GCMs data are shown in Figure 4.5 and 4.6 and also tabulated in Table 4.2.

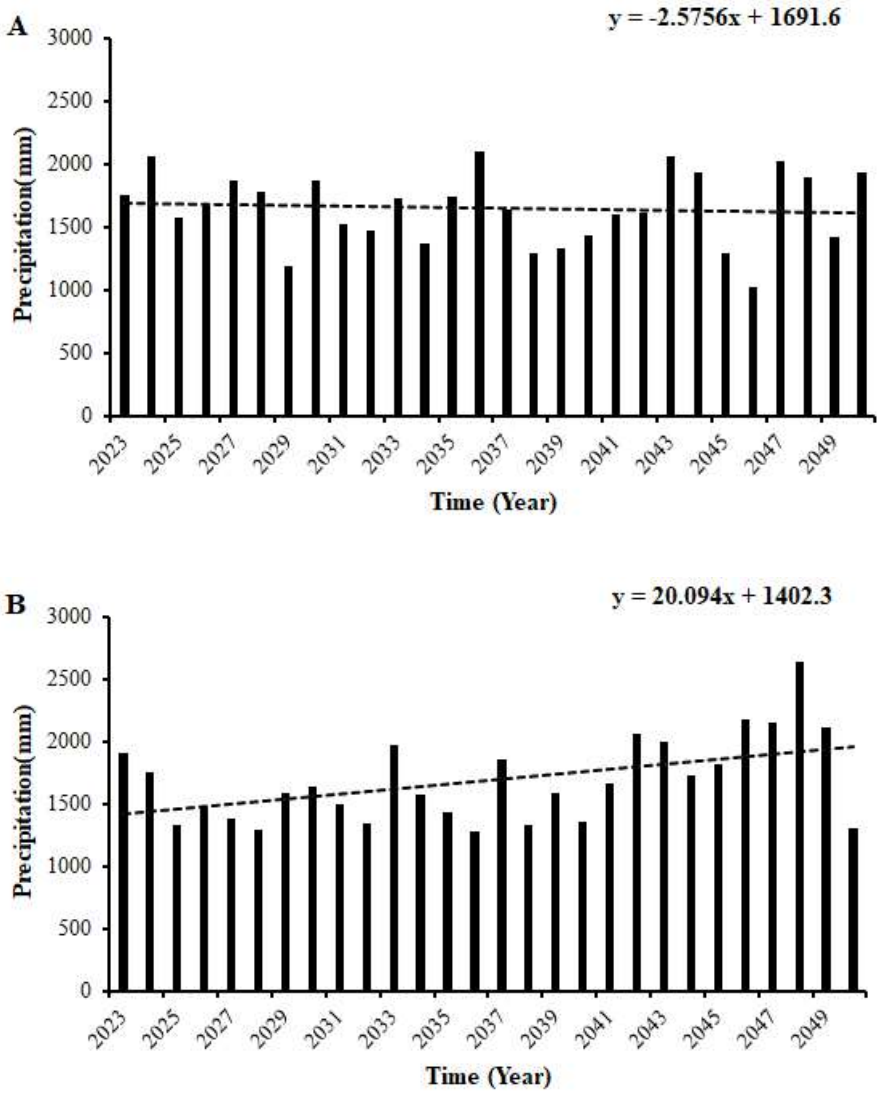

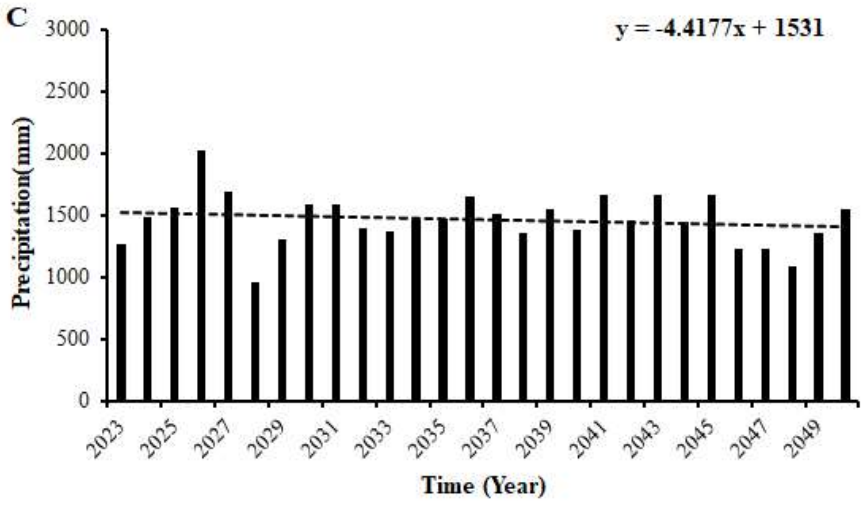
C
y = -4.4177x + 1531
Precipitation(mm)
3000
2500
2000
1500
1000
500
0
2023
2025
2027
2029
2031
2033
2035
2037
2039
2041
2043
2045
2047
2049
Time (Year)

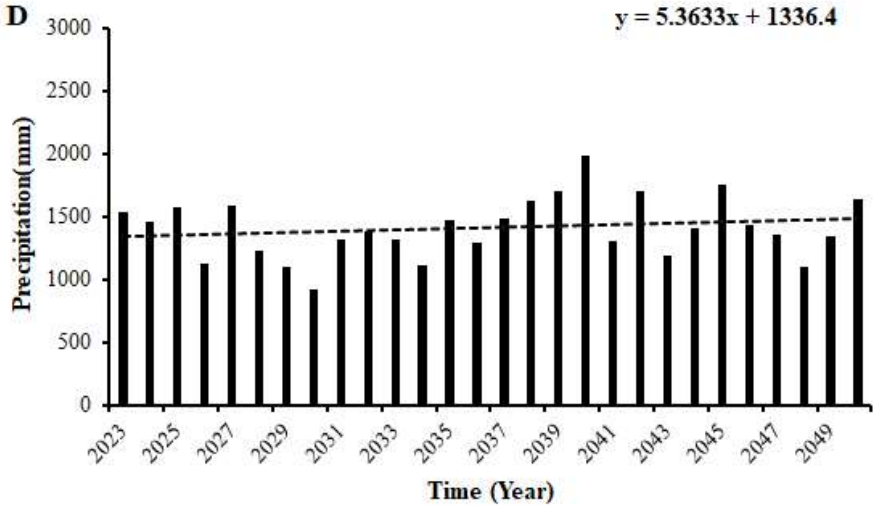
D
y = 5.3633x + 1336.4
Precipitation(mm)
3000
2500
2000
1500
1000
500
0
2023
2025
2027
2029
2031
2033
2035
2037
2039
2041
2043
2045
2047
2049
Time (Year)

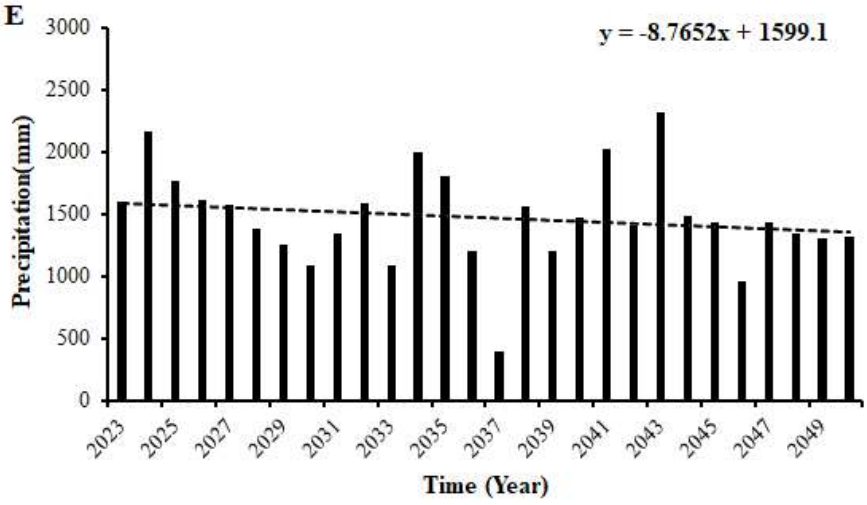
E
y = -8.7652x + 1599.1
Precipitation(mm)
3000
2500
2000
1500
1000
500
0
2023
2025
2027
2029
2031
2033
2035
2037
2039
2041
2043
2045
2047
2049
Time (Year)

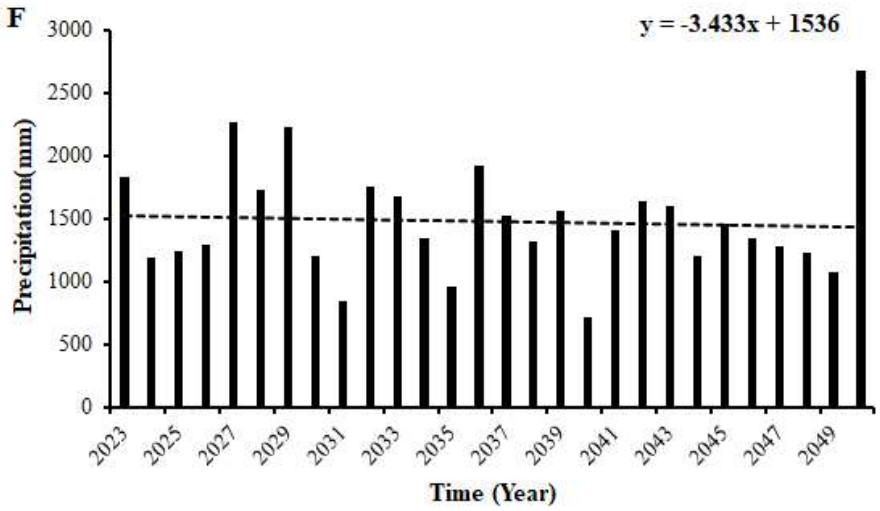

Figure 0.5 (A) Future total annual precipitation variation under EC-Earth3 GCM SSP 245 scenario (2023-2050) (B) Future total annual precipitation variation under EC-Earth3 GCM SSP 585 scenario (2023-2050) (C) Future total annual precipitation variation under MPI-ESM1-2-HR GCM SSP24.5 scenario (2023-2050) (D) Future total annual precipitation variation under MPI-ESM1-2-HR SSP 585 scenario (2023-2050) (E) Future total annual precipitation variation under Nor ESM2-MM GCM SSP24.5 scenario (2023-2050) (F) Future total annual precipitation variation under Nor ESM2-MM SSP58.5 scenario (2023-2050).

Provocatively, the above shown graph of future projected precipitation from three different GCMs shows the declining trend at the rate of 2.57 mm/year, 4.41 mm/year and 8.76 mm/year in TRB under SSP24.5 scenario as projected by GCM EC-Earth3, MPI-ESM1-2HR and Nor-ESM2-MM respectively. Similarly, under SSP585 Scenarios EC-Earth3 project the increasing trend of at the rate of 20.09 mm/year followed by the rate 5.36 mm/year projected by MPI-ESM1-2HR. Yet under SSP58.5 scenario Nor-ESM2-MM shows the decreasing trend in the precipitation at the rate of 3.43 mm/year. This anticipated reduction in precipitation rates may result in a decline in the simulated discharge in future scenarios.

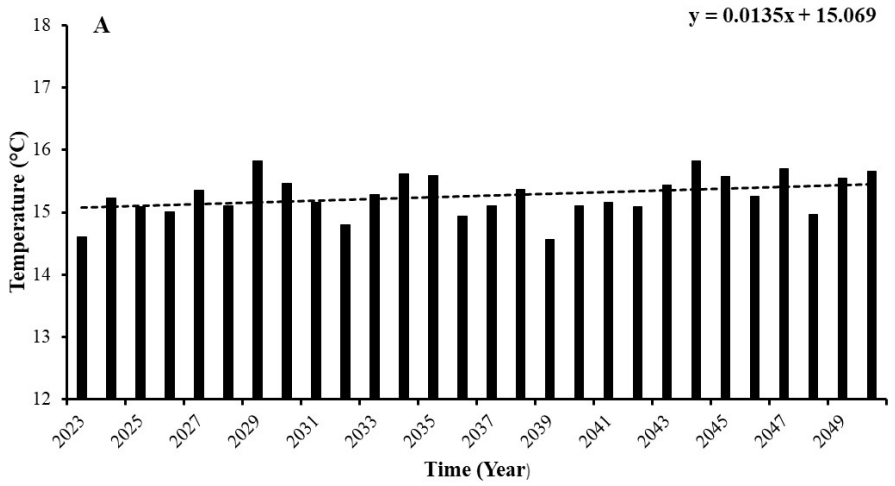
A
y = 0.0135x + 15.069
Temperature (°C)
Time (Year)

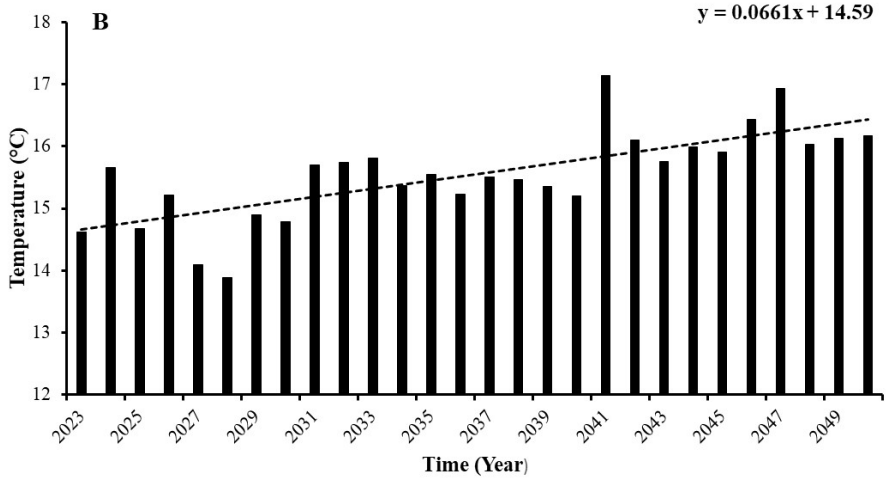
B
y = 0.0661x + 14.59
Temperature (°C)
Time (Year)

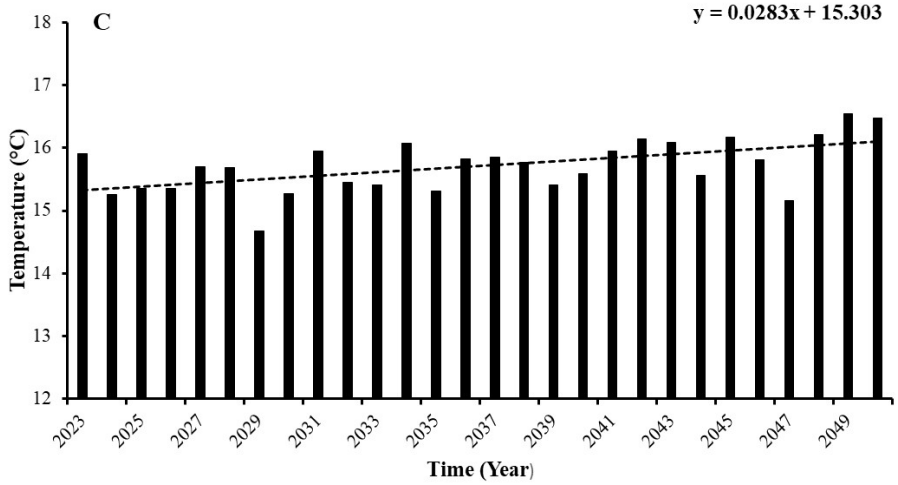
C
y = 0.0283x + 15.303
Temperature (°C)
Time (Year)

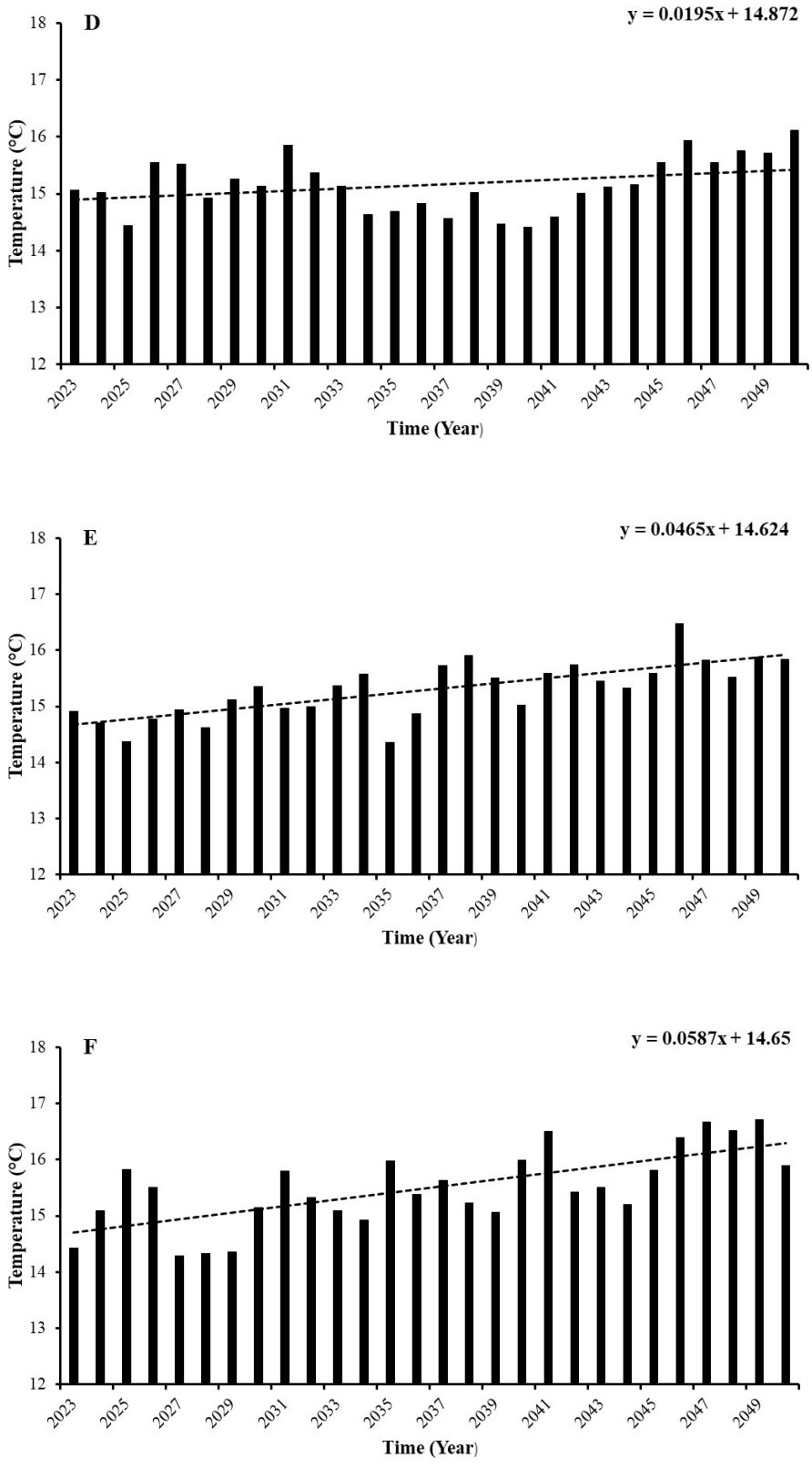

Figure 0.6 (A) Future average annual temperature variation at base station under EC-Earth3 GCM SSP24.5 scenario (2023-2050) (B) Future average annual temperature

variation at base station under EC-Earth3 GCM SSP58.5 scenario (2023-2050) (C) Future average annual temperature variation at base station under MPI-ESM1-2-HR GCM SSP24.5 scenario (2023-2050) (D) Future average annual temperature variation at base station under MPI-ESM1-2-HR SSP58.5 scenario (2023-2050) (E) Future average annual temperature variation at base station under Nor ESM2-MM GCM SSP24.5 scenario (2023-2050) (F) Future average annual temperature variation at base station under Nor ESM2-MM SSP58.5 scenario (2023-2050).

The graphs above shows the increment of temperature at the rate of 0.013 (°C/yr), 0.028 (°C/yr), 0.046 (°C/yr) on SSP24.5 scenario as projected by GCMs EC-Earth3, MPI-ESM1-2HR and Nor-ESM2-MM respectively. Furthermore on SSP58.5 scenario there is the increment of the temperature at the rate of 0.066(°C/yr), 0.019 (°C/yr) and 0.058(°C/yr) by the GCMs sequentially.

Table 0.2 Precipitation and Temperature trend per year up to 2050.

Scenario	GCM	Precipitation Trend (mm/yr)	Temperature Trend (°C/yr)
SSP24.5	EC-Earth3	-2.57	0.013
SSP58.5	EC-Earth3	20.09	0.066
SSP24.5	MPI-ESM1-2-HR	-4.41	0.028
SSP58.5	MPI-ESM1-2-HR	5.36	0.019
SSP24.5	Nor ESM2-MM	-8.76	0.046
SSP58.5	Nor ESM2-MM	-3.43	0.058

4.4 Future Discharge Trend

Using a calibrated and validated model, the future discharge was computed in GDM by inputting future temperature and precipitation data for two SSP scenarios from three different GCMs together with bias correction. In the SSP24.5 scenario, the forecasted discharge until 2050 demonstrates an increase at a rate of 0.30 m^3s^{-1} and a decrease at a rate of 1.9 m^3s^{-1}, 0.09 m^3s^{-1}based on data from EC-Earth3, MPI-ESM1-2HR, and Nor-ESM2-MM, respectively. Conversely, in SSP58.5, discharge is projected to rise at rates of 3.68 m^3s^{-1}, 0.56 m^3s^{-1}, and 0.19 m^3s^{-1} for the same models (Table 4.3). Notably, ice melt consistently outpaces snowmelt in contributing to the overall discharge, showing an upward trend in ice melting year by year and day by day. Surprisingly, the portion of baseflow contributing to total discharge does not exhibit a significant upward pattern. Upon analyzing the various contributors, the average contributions stand at 31.78% for

baseflow, 8.85% for ice melt, 53.65% for rainfall, and 5.7% for snowmelt. Rainfall maintains its prominence as the primary contributor to overall discharge. Intriguingly, in the SSP58.5 scenario, contributions from all components display a clear rising trend. Examining the different elements, baseflow averages at 31.69%, ice melt at 15.03%, rainfall at 48.03%, and snowmelt at 5.2%. Notably, snowmelt appears less impactful, while ice melt is more prominent than in the SSP24.5 scenario, possibly due to increasing daily temperatures, whereas rainfall exhibits a noticeable upward trend.

For the MPI-ESM1-2HR in the SSP24.5 scenarios, there is a slight decline in the simulated total discharge trend, aligning with a diminishing trend in rainfall contribution, while baseflow remains relatively stable. Contributors include baseflow at 33.47%, ice melt at 12.99%, rainfall at 46.71%, and snowmelt at 6.8%. In SSP58.5 scenarios, no significant trends are observed in baseflow, rain, or snowmelt. However, ice melt shows a slight increasing trend, with contributors remaining consistent: baseflow at 31.33%, ice melt at 19.06%, rainfall at 43.74%, and snowmelt at 5.85%. Under the SSP24.5 scenarios, Nor-ESM2-MM indicates a decrease, aligning with a declining trend in rainfall contribution, stable baseflow, and a slight increase in snowmelt. Contributors include baseflow at 32.07%, ice melt at 11.83%, rainfall at 50.67%, and snowmelt at 5.4%. In SSP58.5 scenarios, no significant trends are noted in baseflow, rain, snowmelt, or ice melt, with contributors suggesting baseflow averages at 31.82%, ice melt at 12.58%, rainfall at 49.04%, and snowmelt at 6.54% (Table 4.4 and Figure 4.7).

Table 0.3 Future Discharge trend in two different scenarios (SSP24.5 and SSP 58.5) by the data provided by three different GCMs

Scenario	GCM	Discharge Trend (m^3/s)
SSP24.5	EC-Earth3	0.30
SSP58.5	EC-Earth3	3.68
SSP24.5	MPI-ESM1-2-HR	-0.19
SSP58.5	MPI-ESM1-2-HR	0.56
SSP24.5	Nor ESM2-MM	-0.09
SSP58.5	Nor ESM2-MM	0.19

Table 0.4 Contribution of different hydrological components for future period i.e. 2050 in two different scenarios from the climatic data given by three different GCMs.

Scenario	GCM	Rainfall (%)	Baseflow (%)	Icemelt (%)	Snowmelt (%)
SSP24.5	EC-Earth3	53.65	31.78	8.85	5.7
SSP58.5	EC-Earth3	48.03	31.69	15.03	5.2
SSP24.5	MPI-ESM1-2-HR	46.71	33.47	12.99	6.8
SSP58.5	MPI-ESM1-2-HR	43.74	31.33	19.006	5.85
SSP24.5	Nor ESM2-MM	50.67	32.07	11.83	5.4
SSP58.5	Nor ESM2-MM	49.04	31.82	12.58	6.54

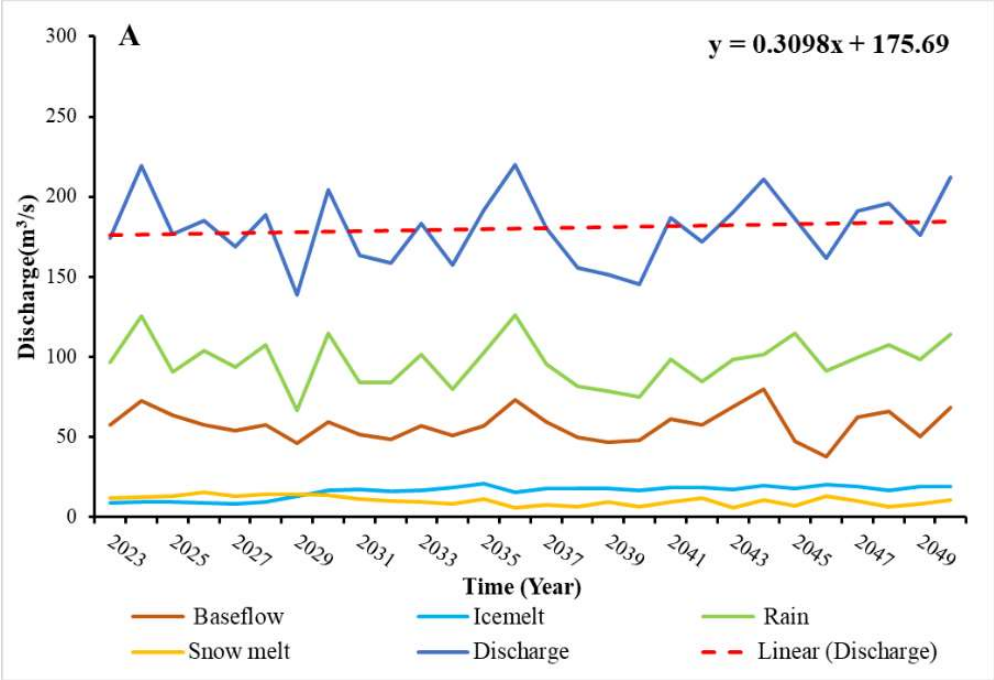

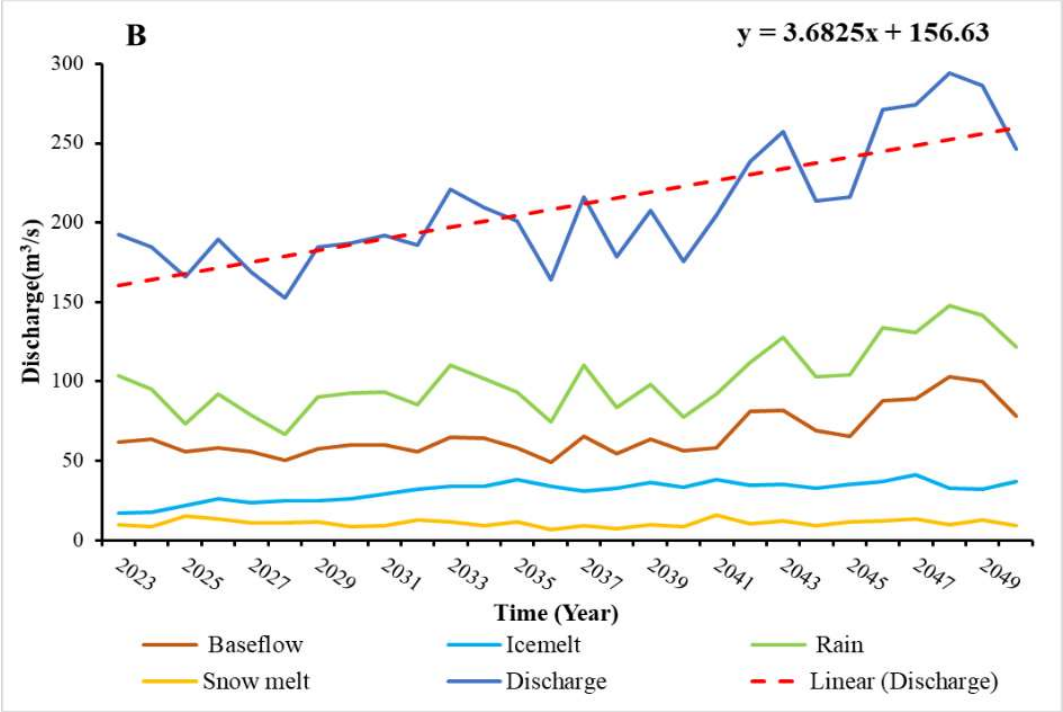
B
y = 3.6825x + 156.63
Discharge(m³/s)
300
250
200
150
100
50
0
2023
2025
2027
2029
2031
2033
2035
2037
2039
2041
2043
2045
2047
2049
Time (Year)
Baseflow
Icemelt
Rain
Snow melt
Discharge
Linear (Discharge)

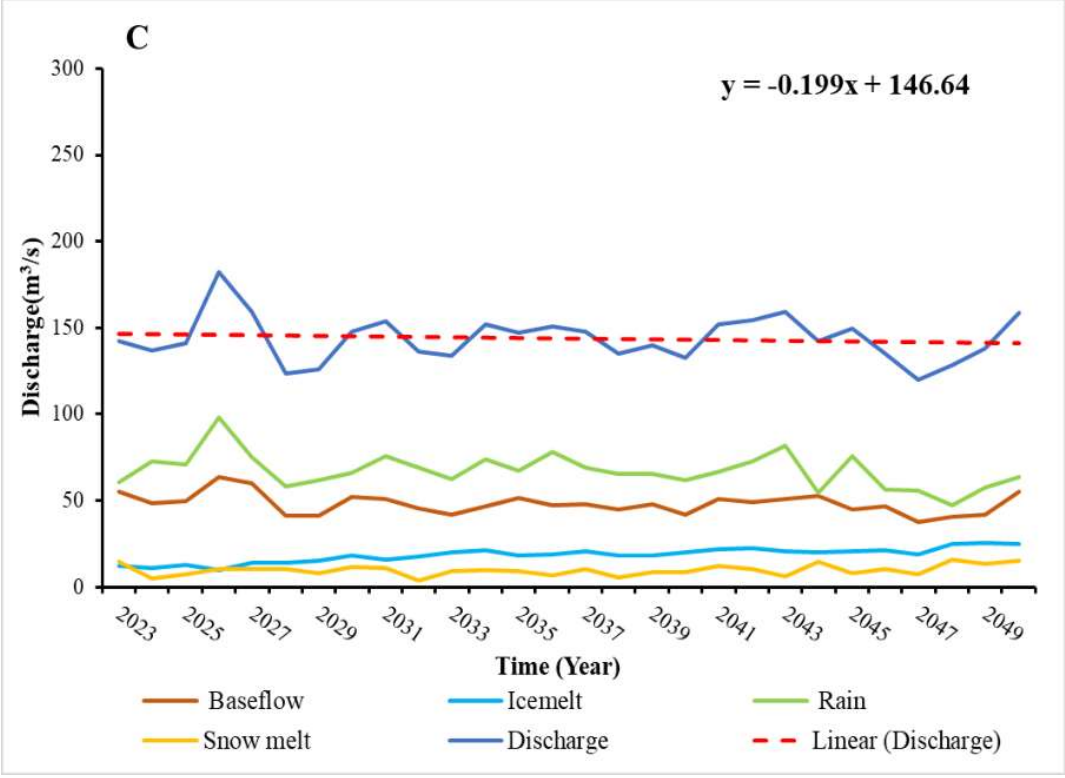
C
y = -0.199x + 146.64
Discharge(m³/s)
300
250
200
150
100
50
0
2023
2025
2027
2029
2031
2033
2035
2037
2039
2041
2043
2045
2047
2049
Time (Year)
Baseflow
Icemelt
Rain
Snow melt
Discharge
Linear (Discharge)

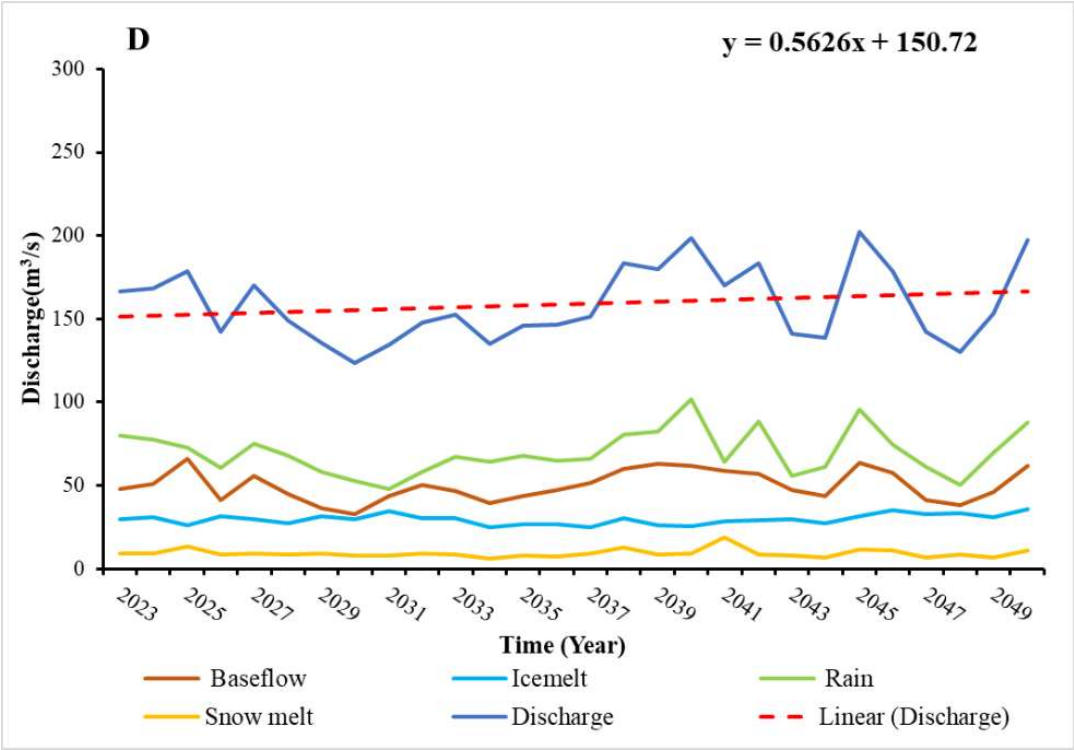
D
y = 0.5626x + 150.72
Discharge(m³/s)
300
250
200
150
100
50
0
2023
2025
2027
2029
2031
2033
2035
2037
2039
2041
2043
2045
2047
2049
Time (Year)
Baseflow
Icemelt
Rain
Snow melt
Discharge
Linear (Discharge)

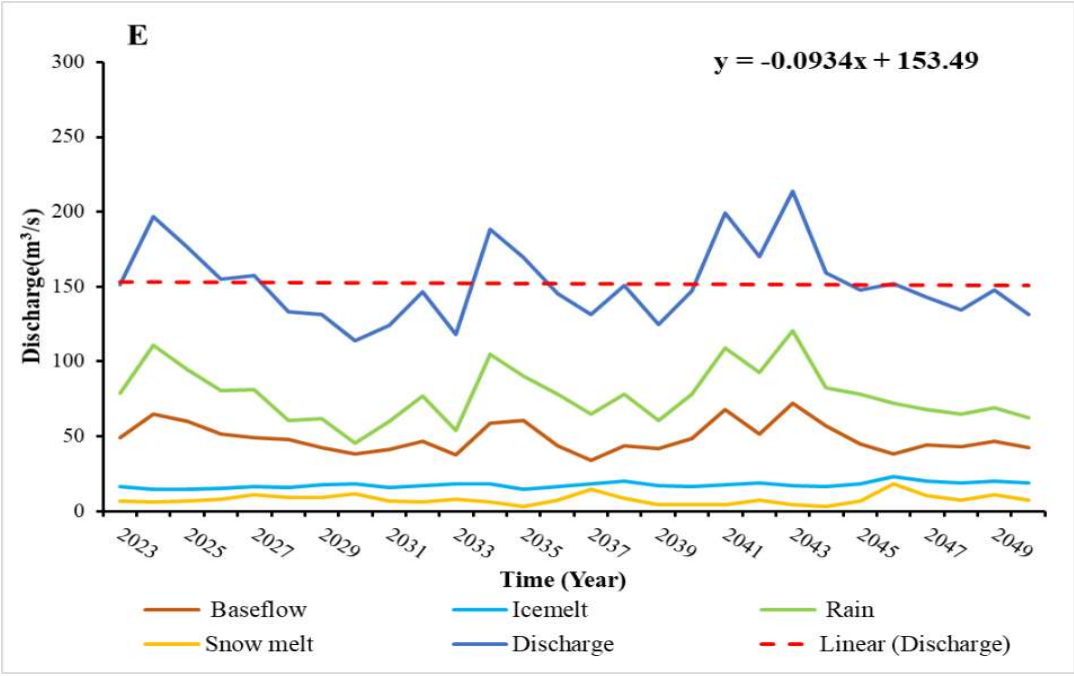
E
y = -0.0934x + 153.49
Discharge(m³/s)
300
250
200
150
100
50
0
2023
2025
2027
2029
2031
2033
2035
2037
2039
2041
2043
2045
2047
2049
Time (Year)
Baseflow
Icemelt
Rain
Snow melt
Discharge
Linear (Discharge)

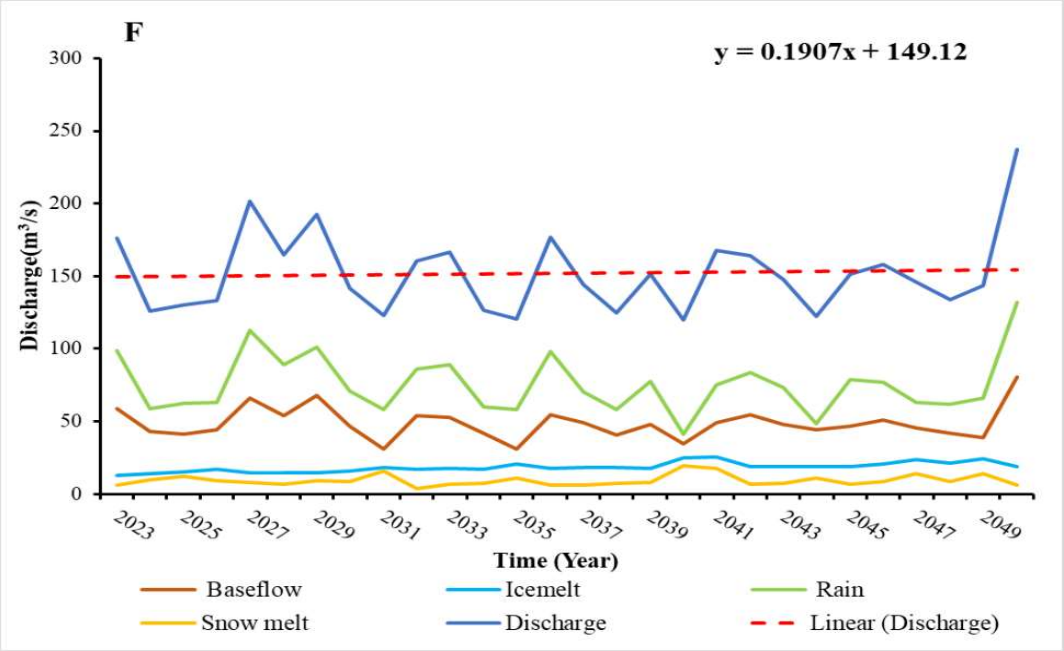

Figure 0.7 (A) Average annual contribution in future discharge under EC-Earth3 GCM SSP24.5 scenario (2023-2050) (B) Average annual contribution in future discharge under EC-Earth3 GCM SSP58.5 scenario (2023-2050) (C) Average annual contribution in future discharge under MPI-ESM1-2-HR GCM SSP24.5 scenario (2023-2050) (D) Average annual contribution in future discharge under MPI-ESM1-2-HR SSP58.5 scenario (2023-2050) (E) Average annual contribution in future discharge under Nor ESM2-MM GCM SSP24.5 scenario (2023-2050) (F) Average annual contribution in future discharge under Nor ESM2-MM SSP58.5 scenario (2023-2050).

When evaluating (Figure 4.8 and 4.9) the monthly average contribution percentage to total discharge, the contribution of icemelt significantly rises from low flow to high flow month i.e. May to June and July under the SSP24.5 and SSP58.5 scenarios by 2050. Notably, icemelt consistently surpasses snowmelt in its contribution to overall discharge, indicating a continuous upward trend in ice melting on both an annual and daily basis. This trend is indicative of potential challenges, given the anticipated increase in temperature leading to reduced snowfall and greater ice melt, resulting in a decline in glacier coverage. This poses a significant threat to the Himalayas and its water system in the foreseeable future.

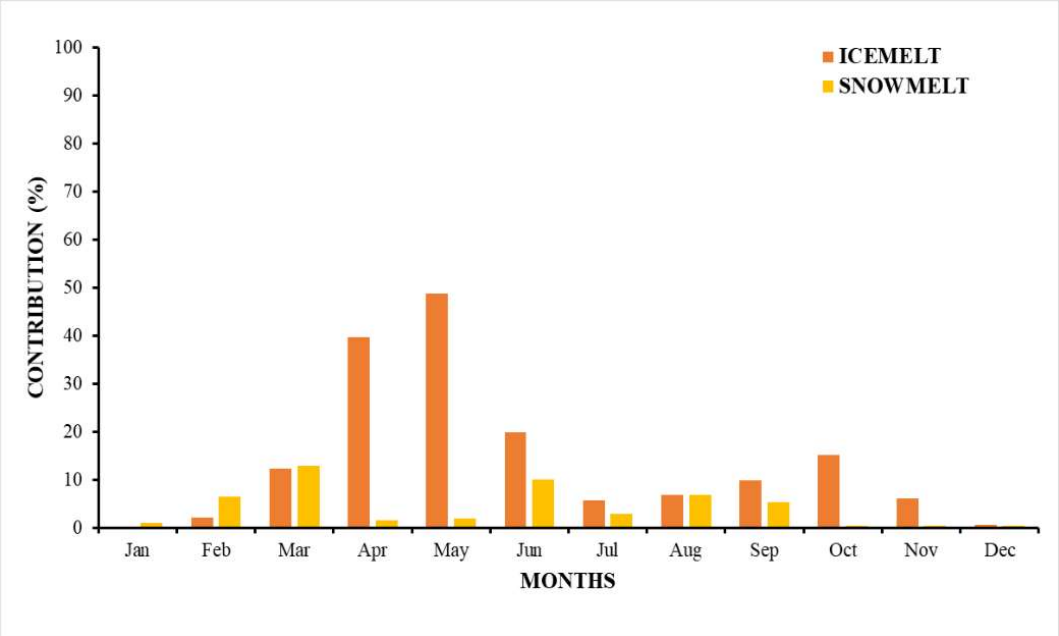

Figure 0.8 Average Monthly Contribution graph of Snowmelt and Icemelt under SSP24.5 (2023-2050) from the obtained data of EC-Earth3 GCM

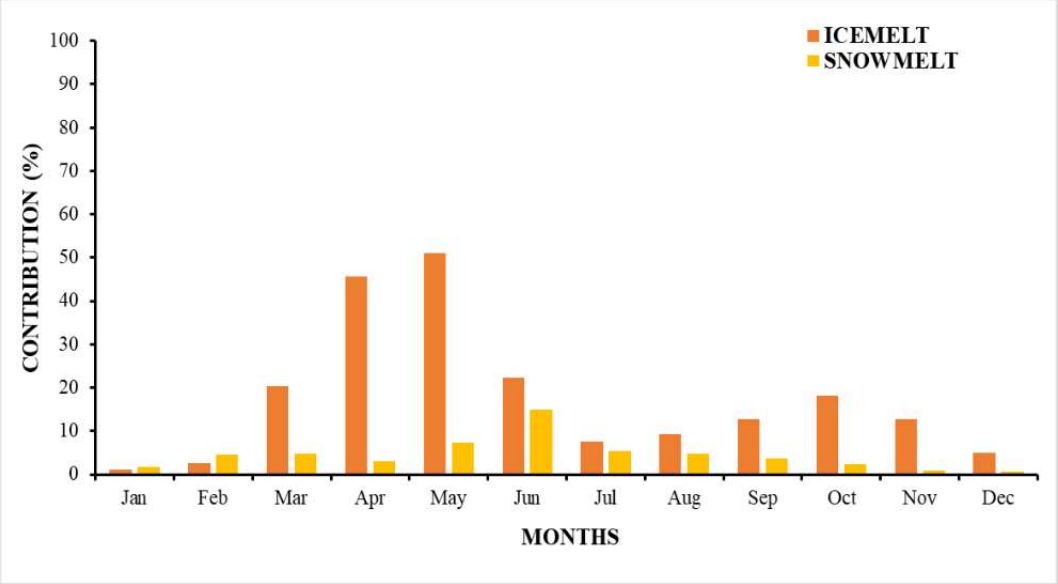

Figure 0.9 Average Monthly Contribution graph of Snowmelt and Icemelt under SSP58.5 (2023-2050) from the obtained data of EC-Earth3 GCM

Figures 4.10 and 4.11 reveal noteworthy insights into the fluctuating patterns of peak discharge. In the SSP24.5 scenario, peak discharge aligns with the baseline period in August from 2023 to 2030, yet shifts to July, surpassing previous years' values from 2031 to 2040. From 2041 to 2050, the peak remains similar to earlier years but with elevated

discharge values. Similarly, in SSP58.5 scenarios, the peak discharge transitions from August to July with increased values post-2030. The fluctuating peak values underscore the significant impact of varying components over different time frames, a phenomenon primarily attributed to climate change.

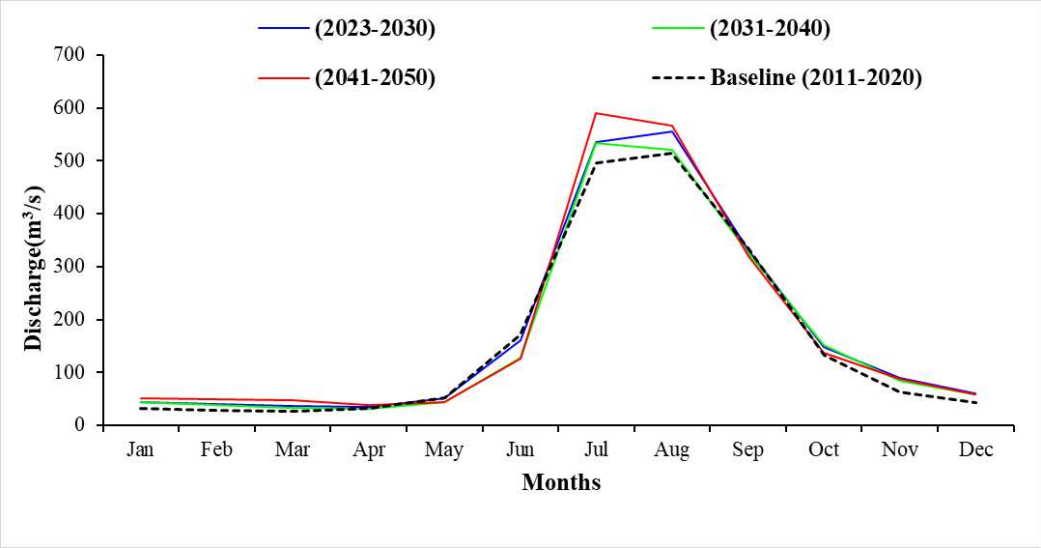

Figure 0.10 Monthly average simulated discharge during reference time period 2023-2030, 2031-2040 and 2041-2050 under SSP24.5 from the obtained data of EC-Earth3 GCM.

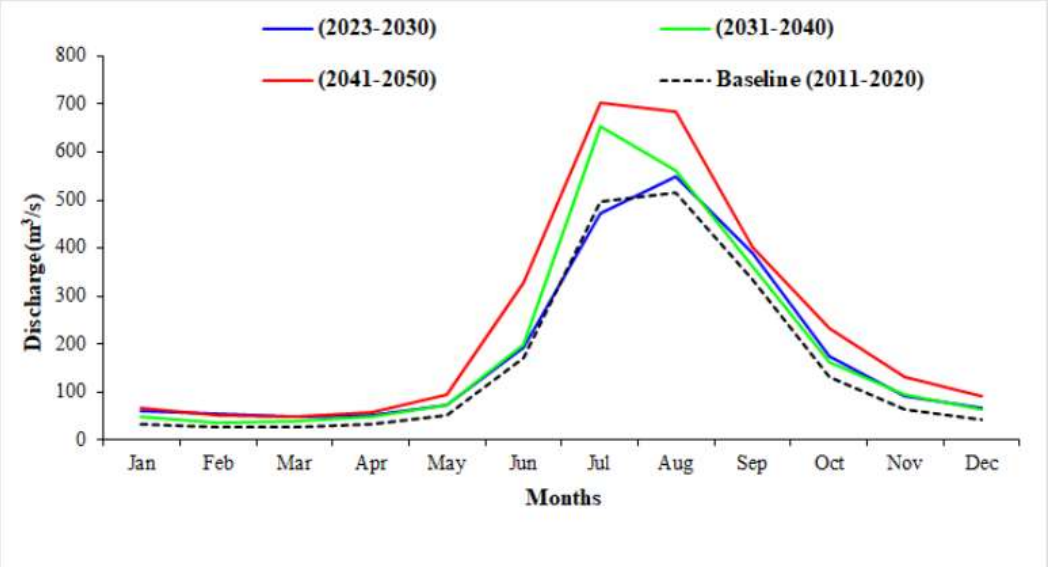

Figure 0.11 Monthly average simulated discharge during reference time period 2023-2030, 2031-2040 and 2041-2050 under SSP58.5 from the obtained data of EC-Earth3 GCM.

Snowmelt, icemelt, rain, and base flow variations according to three GCMs are displayed in Figure 4.12, here in the monthly average contribution the rain fall dominates the contribution followed by the base flow throughout the year. Here from the graph we have comparing the result of three different GCMs the EC-Earth3 GCM shows a bit higher value of contribution especially from June to September. We also have the Gilgit river basin is experiencing the highest rate of glacier melting i.e. about 45% (Adnan et al., 2022). Throughout all General Circulation Model (GCM) forecasts, spanning June to September, rain consistently emerges as the predominant contributor to stream flow, trailed by base flow, snowmelt, and ice melt. Beyond October, base flow takes precedence, and ice melt is prominent between April and October across all three GCMs. In both SSP24.5 and SSP58.5 scenarios, MPI-ESM1-2HR and Nor ESM2-MM exhibit similar substantial variations in key hydrological parameters.

However, in the SSP58.5 scenario with EC-Earth3, total discharge surpasses that of SSP24.5 due to distinctions in contributing components to stream flow ranges. Rainfall and base flow persist as the primary stream flow sources across all three GCM projections. Upon comparing our findings with the study conducted on the Koshi river basin by (M. Khadka et al., 2020), a decline in snowmelt contribution to stream flow is evident. This aligns with diminishing snow-covered areas and storage capacity attributed to rising temperatures, resulting in reduced future snowmelt. In the Tamakoshi basin, ice melt contributions seem to diminish in the RCP 8.5 scenario compared to RCP 4.5 across most seasons, potentially due to a substantial reduction in glacier area. Our study's ice melt contribution appears stable, perhaps owing to a delay in considering changes in glacier area retreat over time, as emphasized in recommendations for future research. The research indicates a significant reduction in glacier area across all sub-basins, yet anticipates a noteworthy ice melt contribution in the future, signaling rapid melting that could lead to the complete disappearance of glaciers (Khadka et al., 2020).

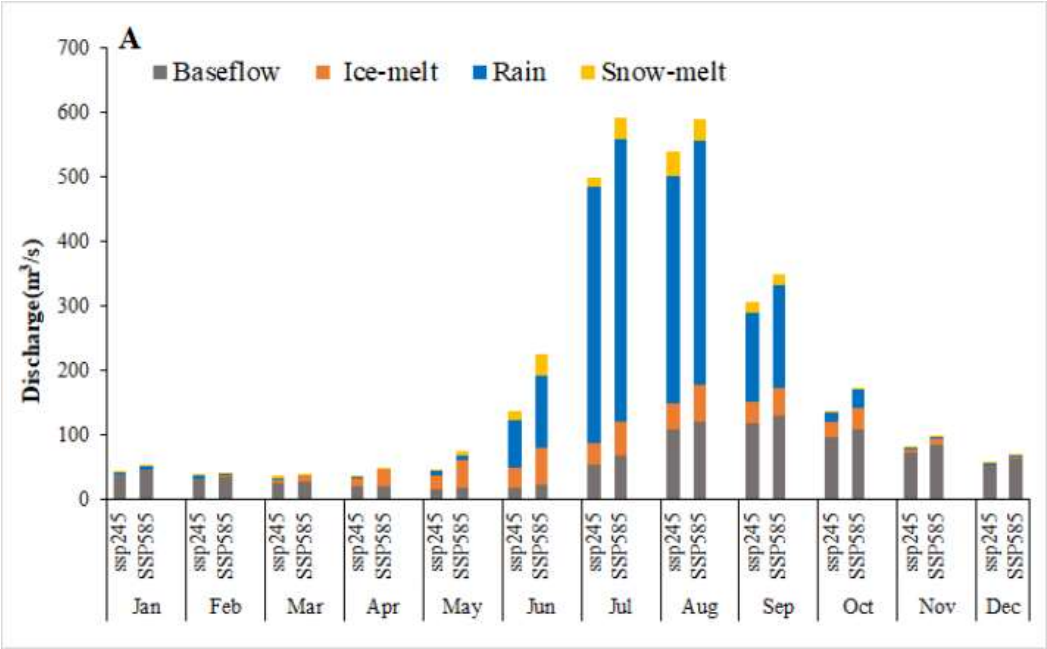
A
Baseflow
Ice-melt
Rain
Snow-melt
Discharge(m³/s)
0
100
200
300
400
500
600
700
ssp245
SSP585
Jan
Feb
Mar
Apr
May
Jun
Jul
Aug
Sep
Oct
Nov
Dec

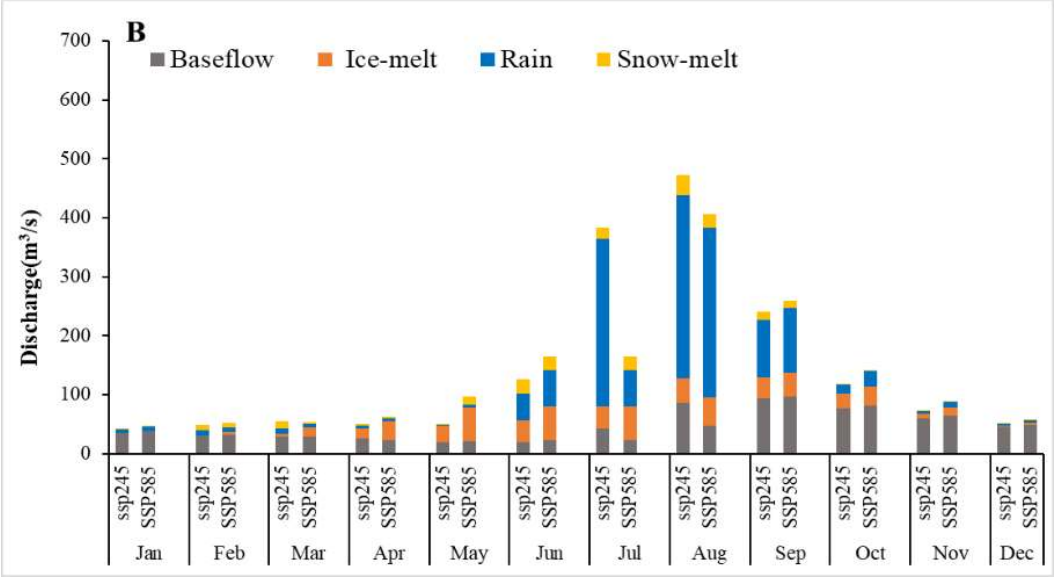
B
Baseflow
Ice-melt
Rain
Snow-melt
Discharge(m³/s)
0
100
200
300
400
500
600
700
ssp245
SSP585
Jan
Feb
Mar
Apr
May
Jun
Jul
Aug
Sep
Oct
Nov
Dec

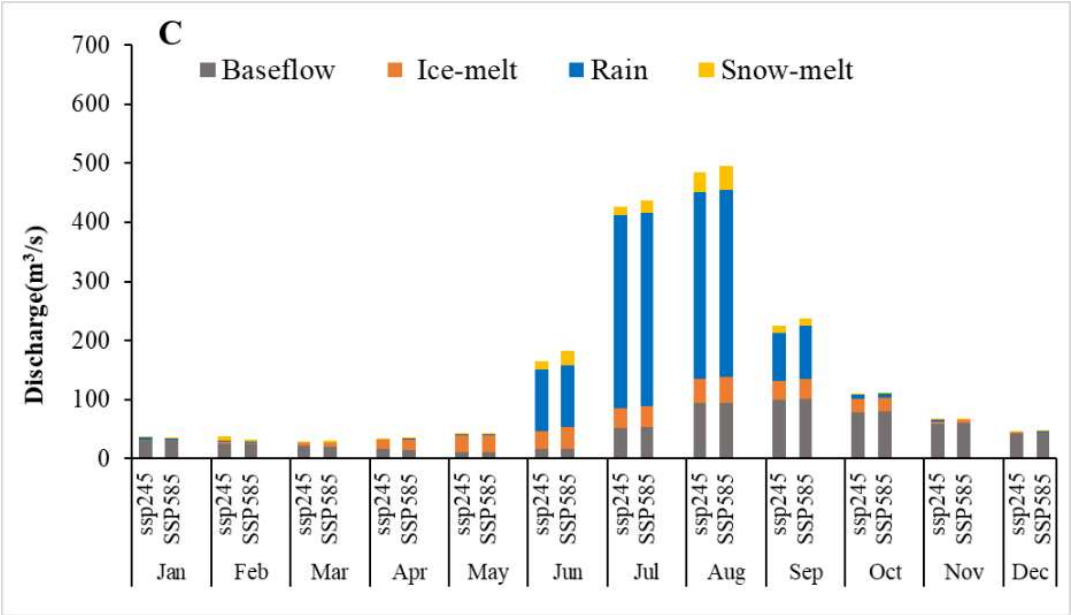

Figure 0.12 (A) Average monthly contribution of hydrological components on discharge in SSP24.5 And SSP58.5 scenarios project by GCM EC-Earth3 for the period (2023-2050) (B) Average monthly contribution of hydrological components on discharge in SSP24.5 And SSP58.5 scenarios project by GCM MPI-ESM1-2HR for the period (2023-2050). (C) Average monthly contribution of hydrological components on discharge in SSP245 and SSP58.5 scenarios project by GCM Nor ESM2-MM for the period (2023-2050).

CHAPTER FIVE: CONCLUSION AND RECCOMENDATION

5.1 Conclusion

Glacio-hydrological Degree-day Model (GDM) has successfully applied in the Tamakoshi River basin and its hydrological regimes is studied. This model accounts for snowmelt, ice melt, rainfall, and base flow to give important cognizance into hydrological dynamics of basin. Despite being straightforward, mentioned model successfully simulates discharge and exhibits respectable accuracy throughout both the calibration and validation phases. In these stages, the coefficient of determination (R^2) maintains a stable value of 0.77 and 0.82, Volume differences 7.8% and 9.5% and the Nash-Sutcliffe Efficiency (NSE) values for the river basins consistently range from 0.77 to 0.80 for calibration and validation period respectively. During the calibration period (2004-2009), snowmelt accounts for 12.17% of the total annual discharge, ice melt contributes 3.18% (from both clean ice and ice under debris), rainfall contributes 46.86%, and base flow makes up 37.57%. Similarly, in the validation period (2011-2020), snowmelt constitutes 10.77% of the total annual discharge, ice melt contributes 3.27% (from both clean ice and ice under debris), rainfall contributes 46.33%, and base flow makes up 38.79%. According to our research, the contribution of snow and glacier melting to overall stream flow height in the monsoon season, while winter has negligible flow. Similarly the rain dominates the contribution in monsoon period which is followed by base flow contribution and the base flow contribution is throughout the whole year within the calibration and validation period during the low-flow period in May to June, substantial contributions from icemelt and snowmelt to stream runoff are evident. This holds true in both calibration and validation periods, emphasizing the significance of these processes. Looking ahead, the diminishing snow and ice in the basin may reduce their contributions, leading to a decline in discharge in the Tamakoshi River basin. Across diverse scenarios, there are distinct variations in temperature and precipitation trends observed among models. In SSP24.5, temperature increases vary between models, with EC-Earth3 indicating a subtle upward trend of 0.013°C/year, MPI-ESM1-2HR at 0.028°C/year, and Nor-ESM2-MM at 0.046°C/year. Conversely, in SSP58.5, EC-Earth3 anticipates a climb at 0.066°C/year, MPI-ESM1-2HR maintains a rate of 0.019°C/year, and Nor-ESM2-MM displays a 0.058°C/year increase. These trends have the potential to impact forthcoming contributions from snowmelt and ice melt. Projections for future water scenarios reveal an uptick in discharge under SSP58.5 and a reduction under SSP24.5. SSP58.5 projects elevated discharge values (e.g.,

3.68 m3/s under EC-Earth3), while SSP24.5 anticipates declines (e.g., 0.19 m3/s under MPI-ESM1-2HR). These shifts likely result from alterations in precipitation and temperature within the respective scenarios. Within different socio-environmental pathways (SSP24.5 and SSP58.5), the constituent contributions to discharge exhibit notable variations. In SSP24.5, baseflow ranges from 31.78% to 33.47%, icemelt from 8.85% to 12.99%, rainfall from 46.71% to 53.65%, and snowmelt from 5.4% to 6.8%. SSP58.5 reveals subtle changes in baseflow, an increase in icemelt (11.83% to 19.006%), stable rainfall (43.74% to 49.04%), and snowmelt proportions (5.2% to 6.54%). The monthly average contribution of icemelt significantly rises from low-flow to high-flow months under the SSP24.5 and SSP58.5 scenarios by 2050, consistently surpassing snowmelt in overall discharge. This upward trend poses challenges due to the anticipated temperature increase, leading to reduced snowfall, increased ice melt, and a decline in glacier coverage, threatening the Himalayas and its water system. Additionally, the shifting peak discharge patterns observed in SSP24.5 and SSP58.5 scenarios highlight the significant impact of changing components over different time frames, primarily influenced by climate change. These findings underscore potential alterations in resource availability and distribution across distinct future socio-environmental pathways.

In conclusion, the Glacio hydrological Degree-day Model (GDM) emerges as a promising tool for comprehending hydrological system dynamics and evaluating the impacts of climate change on Himalayan river basins.

5.2 Recommendation

1. Combining the Glacier Dynamic Model (GDM) with the Open Global Glacier Model (OGGM) improves accuracy through the incorporation of OGGM data, offering detailed information on annual glacier retreat rates and variations in clean and debris-covered ice within the basin.
2. Performing an Isotope test is a valuable method to examine the contributions of rain, snowmelt, ice melt, and baseflow to the stream flow in the basin.
3. To comprehensively grasp and predict climate change impacts in the Himalayan region, particularly on downstream water availability, essential research should extend to multiple basins across the northern and southern slopes too.

CHAPTER SIX: REFERENCES

Acharya, S., & Sellmyer, A. (n.d.). 24; nabin Baral-pp 26, 34; narendra Raj Khanel-p 22; nlC, Bhutan-p 17; practical Action-p 14; Santosh pathak-p 16; Seema Karki-p 23; Shikhar Bhattarai-p 49; Subasana Shrestha-p 47; ujol Sherchan-p 41. In *Juerg Merz-p* (Vol. 1). www.icimod.org/himaldoc

Adhikari, T. R., Talchabhadel, R., Shrestha, S., Sharma, S., Aryal, D., & Pradhanang, S. M. (2022). The evaluation of climate change impact on hydrologic processes of a mountain river basin. *Theoretical and Applied Climatology*, *150*(1–2), 749–762. https://doi.org/10.1007/S00704-022-04204-3/METRICS

Adnan, M., Liu, S., Saifullah, M., Iqbal, M., Ali, A. F., & Mukhtar, M. A. (2022). Spatiotemporal variations in runoff and runoff components in response to climate change in a glacierized subbasin of the Upper Indus Basin, Pakistan. *Frontiers in Earth Science*, *10*(August), 1–20. https://doi.org/10.3389/feart.2022.970349

Apollo, M. (n.d.). *The population of Himalayan regions-by the numbers: Past, present and future Special Issue of Frontiers in Sustainable Tourism: Tourism Development, Sustainability, and Inclusion View project*. https://www.researchgate.net/publication/313849476

Arnold, J. G., Srinivasan, R., Muttiah, R. S., & Williams2, J. R. (1998). Large Area Hydrologic Modeling and Assessment Part I: Model Development'. *Journal of the American Water Resources Association*, *34*(1), 73–89.

Aryal, A., Shrestha, S., & Babel, M. S. (2019). Quantifying the sources of uncertainty in an ensemble of hydrological climate-impact projections. *Theoretical and Applied Climatology*, *135*(1–2), 193–209. https://doi.org/10.1007/s00704-017-2359-3

Bergdtrom Sten, Caelsson Bengt, Gardelin Marie, Lindstorm Goran, Pettersson Anna, & Rummukainen. (n.d.). *CLIMATE RESEARCH Clim Res*.

Bergström, S. (1992). The HBV model - its structure and applications. *Swedish Meteorological and Hydrological Institute, Norrköping*, *4*(4), 1–33.

Braithwaite, R. J. (1995). Positive Degree-Day Factors for Ablation on the Greenland Ice-Sheet Studied by Energy-Balance Modeling. *Journal of Glaciology*, *41*(137), 153–160. https://research.manchester.ac.uk/en/publications/positive-degree-day-factors-for-ablation-on-the-greenland-ice-she

Braithwaite, R. J., & Olesen, O. B. (1989). *Calculation of glacier ablation from air temperature, West Greenland* (pp. 219–233). Kluwer Academic Publishers. https://research.manchester.ac.uk/en/publications/calculation-of-glacier-ablation-from-air-temperature-west-greenla

Budhathoki, B. R., Adhikari, T. R., Shrestha, S., & Awasthi, R. P. (2023). Application of hydrological model to simulate streamflow contribution on water balance in Himalaya river basin, Nepal. *Frontiers in Earth Science*, *11*(May), 1–11. https://doi.org/10.3389/feart.2023.1128959

Carnicer, J., Coll, M., Ninyerola, M., Pons, X., Sánchez, G., & Peñuelas, J. (2011). Widespread crown condition decline, food web disruption, and amplified tree mortality with increased climate change-type drought. *Proceedings of the National Academy of Sciences of the United States of America*, *108*(4), 1474–1478.

https://doi.org/10.1073/pnas.1010070108

Consortium, R. (2023). *Randolph Glacier Inventory - A Dataset of Global Glacier Outlines, Version 6 [Data Set]*. https://doi.org/10.7265/4m1f-gd79

Cunderlik, J. M., Simonovic, S. P., Mcbean, G., Burn, D. H., Mortsch, L., Goldt, R., & Helsten, M. (2003). *Hydrologic model selection for the CFCAS project: Assessment of Water Resources Risk and Vulnerability to Changing Climatic Conditions Prepared by Upper Thames River Conservation Authority*.

da Silva, M. G., de Aguiar Netto, A. de O., de Jesus Neves, R. J., do Vasco, A. N., Almeida, C., & Faccioli, G. G. (2015). Sensitivity Analysis and Calibration of Hydrological Modeling of the Watershed Northeast Brazil. *Journal of Environmental Protection*, *06*(08), 837–850. https://doi.org/10.4236/jep.2015.68076

Daigneault, A., Johnston, C., & Baker, J. S. (2018). *Developing Detailed Shared Socioeconomic Pathway (SSP) Narratives for the Global Forest Sector Global Forest Biodiversity Initiative View project Modelling and Informing Low-Emission Strategies View project*. https://www.researchgate.net/publication/328582860

De Jong, C., Collins, D. (David N. ., & Ranzi, R. (2005). *Climate and hydrology in mountain areas*. Wiley.

Devkota, L. P., & Gyawali, D. R. (2015). Impacts of climate change on hydrological regime and water resources management of the Koshi River Basin, Nepal. *Journal of Hydrology: Regional Studies*, *4*, 502–515. https://doi.org/10.1016/j.ejrh.2015.06.023

Ghimire, U., Babel, M. S., Shrestha, S., & Srinivasan, G. (2019). A multi-temporal analysis of streamflow using multiple CMIP5 GCMs in the Upper Ayerawaddy Basin, Myanmar. *Climatic Change*, *155*(1), 59–79. https://doi.org/10.1007/s10584-019-02444-3

Hassan, J., Chen, X. qing, Kayastha, R. B., & Nie, Y. (2021). Multi-model assessment of glacio-hydrological changes in central Karakoram, Pakistan. *Journal of Mountain Science*, *18*(8), 1995–2011. https://doi.org/10.1007/s11629-021-6748-9

Hirabayashi, Y., Mahendran, R., Koirala, S., Konoshima, L., Yamazaki, D., Watanabe, S., Kim, H., & Kanae, S. (2013). Global flood risk under climate change. *Nature Climate Change*, *3*(9), 816–821. https://doi.org/10.1038/nclimate1911

Hock, R. (1999). A distributed temperature-index ice- and snowmelt model including potential direct solar radiation. *Journal of Glaciology*, *45*(149), 101–111. https://doi.org/10.3189/s0022143000003087

Hock, R. (2003). Temperature index melt modelling in mountain areas. *Journal of Hydrology*, *282*(1–4), 104–115. https://doi.org/10.1016/S0022-1694(03)00257-9

Immerzeel, W. W., Pellicciotti, F., & Bierkens, M. F. P. (2013). Rising river flows throughout the twenty-first century in two Himalayan glacierized watersheds. *Nature Geoscience*, *6*(9), 742–745. https://doi.org/10.1038/ngeo1896

Immerzeel, W. W., Wanders, N., Lutz, A. F., Shea, J. M., & Bierkens, M. F. P. (2015). Reconciling high-altitude precipitation in the upper Indus basin with glacier mass balances and runoff. *Hydrology and Earth System Sciences*, *19*(11), 4673–4687. https://doi.org/10.5194/hess-19-4673-2015

Intergovernmental Panel on Climate Change (IPCC). (2022). Technical Summary. In *The Ocean and Cryosphere in a Changing Climate* (pp. 39–70). Cambridge University Press. https://doi.org/10.1017/9781009157964.002

IPCC. (2007). *Climate Change 2007: Synthesis Report. Contribution of Working Groups I, II and III to the Fourth Assessment Report of the Intergovernmental Panel on Climate Change*. 104.

Juen, I., Kaser, G., & Georges, C. (2007). Modelling observed and future runoff from a glacierized tropical catchment (Cordillera Blanca, Perú). *Global and Planetary Change*, *59*(1–4), 37–48. https://doi.org/10.1016/j.gloplacha.2006.11.038

Karki, R., Talchabhadel, R., Aalto, J., & Baidya, S. K. (2016). New climatic classification of Nepal. *Theoretical and Applied Climatology*, *125*(3–4), 799–808. https://doi.org/10.1007/s00704-015-1549-0

Karra, & Kontigs. (2021). Global land use/land cover with Sentinel-2 and deep learning. *IEEE International Geoscience and Remote Sensing Symposium*.

Kayastha, R. B. . T. Y. . N. M. . and A. Y. (2000). *Practical prediction of ice melting beneath various thickness of debris cover on Khumbu Glacier, Nepal, using a positive degree-day factor*. https://www.researchgate.net/publication/283837946_Practical_prediction_of_ice_melting_beneath_various_thickness_of_debris_cover_on_Khumbu_Glacier_Nepal_using_a_positive_degree-day_factor

Kayastha, R. B., Ageta, Y., & Nakawo, M. (2000). Positive degree day factors in abalation of Glaciers in Nepelese Himalayas: Case study on Glaciers AX010 in Shorong Himal, Nepal. *IAHS, Publ*, *Wallingford*, 71–81.

Kayastha, R. B., & Kayastha, R. (2019). Glacio-hydrological degree-day model (gdm) useful for the himalayan river basins. In *Himalayan Weather and Climate and their Impact on the Environment* (pp. 379–398). Springer International Publishing. https://doi.org/10.1007/978-3-030-29684-1_19

Kayastha, R. B., Steiner, N., Kayastha, R., Mishra, S. K., & McDonald, K. (2020). Comparative Study of Hydrology and Icemelt in Three Nepal River Basins Using the Glacio-Hydrological Degree-Day Model (GDM) and Observations From the Advanced Scatterometer (ASCAT). *Frontiers in Earth Science*, *7*. https://doi.org/10.3389/feart.2019.00354

Khadka, A., Devkota, L. P., & Kayastha, R. B. (2015). Impact of Climate Change on the Snow Hydrology of Koshi River Basin. In *Journal of Hydrology and Meteorology* (Vol. 9, Issue 1).

Khadka, D., Babel, M. S., Shrestha, S., & Tripathi, N. K. (2014). Climate change impact on glacier and snow melt and runoff in Tamakoshi basin in the Hindu Kush Himalayan (HKH) region. *Journal of Hydrology*, *511*, 49–60. https://doi.org/10.1016/j.jhydrol.2014.01.005

Khadka, D., & Pathak, D. (2016). Climate change projection for the marsyangdi river basin, Nepal using statistical downscaling of GCM and its implications in geodisasters. *Geoenvironmental Disasters*, *3*(1). https://doi.org/10.1186/s40677-016-0050-0

Khadka, M., Kayastha, R. B., & Kayastha, R. (2020). Future projection of cryospheric and hydrologic regimes in Koshi River basin, Central Himalaya, using coupled glacier dynamics and glacio-hydrological models. *Journal of Glaciology*, *66*(259), 831–845. https://doi.org/10.1017/jog.2020.51

Khanal, S., Lutz, A. F., Kraaijenbrink, P. D. A., van den Hurk, B., Yao, T., & Immerzeel, W. W. (2021). Variable 21st Century Climate Change Response for Rivers in High Mountain Asia at Seasonal to Decadal Time Scales. *Water Resources Research*, *57*(5), 1–26. https://doi.org/10.1029/2020WR029266

Knutti, R., Arblaster, J., Dufresne, J., Fichefet, T., Friedlingstein, P., Gao, X., Gutowski, W., Johns, T., Krinner, G., Shongwe, M., Tebaldi, C., Weaver, A., Wehner, M., Qin, D., Plattner, G., Tignor, M., Allen, S., Boschung, J., Nauels, A., … Allen, M. R. (2013). *Mxolisi Shongwe (South Africa), Claudia Tebaldi (USA)*.

Krause, P. (2002). Quantifying the impact of land use changes on the water balance of large catchments using the J2000 model. *Physics and Chemistry of the Earth*, *27*(9–10), 663–673. https://doi.org/10.1016/S1474-7065(02)00051-7

Krause, P., & Kralisch, S. (2005). The hydrological modelling system J2000 - Knowledge core for JAMS. *MODSIM05 - International Congress on Modelling and Simulation: Advances and Applications for Management and Decision Making, Proceedings*, *December 2005*, 676–682.

Li, F., Zhang, G., & Xu, Y. J. (2016). Assessing climate change impacts on water resources in the Songhua River Basin. *Water (Switzerland)*, *8*(10). https://doi.org/10.3390/w8100420

Lima, M. G. B., & Gupta, J. (2013). The policy context of biofuels: A case of non-governance at the global level? *Global Environmental Politics*, *13*(2), 46–64. https://doi.org/10.1162/GLEP_a_00166

Luo, Y., Arnold, J., Allen, P., & Chen, X. (2012). Baseflow simulation using SWAT model in an inland river basin in Tianshan Mountains, Northwest China. *Hydrology and Earth System Sciences*, *16*(4), 1259–1267. https://doi.org/10.5194/hess-16-1259-2012

Lutz Arthur, Immerzeel Water, Biemans Hester, Maat ter Herbert, Veldore Vidyunmala, & Shrestha Arun. (n.d.). *Selection of Climate Models for Developing Representative Climate Projections for the Hindu Kush Himalayan Region Consortium members*. www.hi-aware.org.

Mengistu, D., Bewket, W., Dosio, A., & Panitz, H. J. (2021). Climate change impacts on water resources in the Upper Blue Nile (Abay) River Basin, Ethiopia. *Journal of Hydrology*, *592*. https://doi.org/10.1016/j.jhydrol.2020.125614

Meteorological, S. (2015). *Development and Application of a Conceptual Runoff Model for Scandinavian Catchments by Sten Bergström*. *January 1976*.

Mishra, V., Bhatia, U., & Tiwari, A. D. (2020). Bias-corrected climate projections for South Asia from Coupled Model Intercomparison Project-6. *Scientific Data*, *7*(1). https://doi.org/10.1038/s41597-020-00681-1

MOONEY, S. (2005). Climate Change in Contrasting River Basins–Adaptation Strategies for Water, Food and Environment. *The Journal of Agricultural Science*.

Niroula, N., Kobayashi, K., & Xu, J. (2015). Sunshine duration is declining in nepal across the period from 1987 to 2010. *Journal of Agricultural Meteorology*, *71*(1), 15–23. https://doi.org/10.2480/agrmet.D-14-00025

Piani, C., Haerter, J. O., & Coppola, E. (2010). Statistical bias correction for daily precipitation in regional climate models over Europe. *Theoretical and Applied Climatology*, *99*(1–2), 187–192. https://doi.org/10.1007/s00704-009-0134-9

Reid, T. D., & Brock, B. W. (n.d.). *An energy-balance model for debris-covered glaciers including heat conduction through the debris layer*.

Seibert, J. (2005). HBV light. *HBV Light Version 2 User's Manual*, *November*.

Seibert, J., & Vis, M. J. P. (2012). Teaching hydrological modeling with a user-friendly catchment-runoff-model software package. *Hydrology and Earth System Sciences*, *16*(9), 3315–3325. https://doi.org/10.5194/hess-16-3315-2012

Shea, J. M., Immerzeel, W. W., Wagnon, P., Vincent, C., & Bajracharya, S. (2015). Modelling glacier change in the Everest region, Nepal Himalaya. *Cryosphere*, *9*(3), 1105–1128. https://doi.org/10.5194/tc-9-1105-2015

Singh, P., Haritashya, U. K., Kumar, N., & Singh, Y. (2006). Hydrological characteristics of the Gangotri Glacier, central Himalayas, India. *Journal of Hydrology*, *327*(1–2), 55–67. https://doi.org/10.1016/j.jhydrol.2005.11.060

Terink, W., Lutz, A. F., Simons, G. W. H., Immerzeel, W. W., & Droogers, P. (2015). SPHY v2.0: Spatial Processes in HYdrology. *Geoscientific Model Development*, *8*(7), 2009–2034. https://doi.org/10.5194/gmd-8-2009-2015

van Tiel, M., Stahl, K., Freudiger, D., & Seibert, J. (2020). Glacio-hydrological model calibration and evaluation. *Wiley Interdisciplinary Reviews: Water*, *7*(6). https://doi.org/10.1002/wat2.1483

Vormoor, K., Heistermann, M., Bronstert, A., & Lawrence, D. (2018). Hydrological model parameter (in)stability–"crash testing" the HBV model under contrasting flood seasonality conditions. *Hydrological Sciences Journal*, *63*(7), 991–1007. https://doi.org/10.1080/02626667.2018.1466056

Wegehenkel, M. (n.d.). *Estimating of the impact of land use changes using the conceptual hydrological model THESEUS-a case study*. www.elsevier.com/locate/pce

Wijngaard, R. R., Lutz, A. F., Nepal, S., Khanal, S., Pradhananga, S., Shrestha, A. B., & Immerzeel, W. W. (2017). Future changes in hydro-climatic extremes in the upper indus, ganges, and brahmaputra river basins. *Plos One*. doi:10.1371/journal.%0Apone.0190224

Wuthiwongyothin, S., Kalkan, C., & Panyavaraporn, J. (n.d.). *Evaluating Inverse Distance Weighting and Correlation Coefficient Weighting Infilling Methods on Daily Rainfall Time Series*.

Yang, M., Li, Z., Anjum, M. N., Kayastha, R., Kayastha, R. B., Rai, M., Zhang, X., & Xu, C. (2022). Projection of Streamflow Changes Under CMIP6 Scenarios in the Urumqi River Head Watershed, Tianshan Mountain, China. *Frontiers in Earth Science*, *10*(April), 1–14. https://doi.org/10.3389/feart.2022.857854

Zhang, H., Zhang, F., Zhang, G., Che, T., & Yan, W. (2018). How Accurately Can the Air

Temperature Lapse Rate Over the Tibetan Plateau Be Estimated From MODIS LSTs? *Journal of Geophysical Research: Atmospheres*, *123*(8), 3943–3960. https://doi.org/10.1002/2017JD028243

Paper ID: E1-4

Application of Glacio Hydrological Model for the Simulation of Stream Flow in Glacierized Tamakoshi River Basin, Nepal

Nabin Chaulagain [a], Rijan Bhakta Kayastha [b], Khem Narayan Poudyal [c]

Abstract:

The glaciers and snow-covered areas has been highly influential in the hydrology of the glacierized basin. Long-term water management will become more difficult as a result of climate change, which is anticipated to alter the water availability. Here we have set up Glacio hydrological Degree-day Model Version 2 (GDM V.2) as a hydrological model to simulate the discharge in Tamkoshi River basin (TRB) and quantified various runoff components. The model is first calibrated and validated for the period of 2004-2009 and 2011-2020 respectively where Nash-Sutcliffe Efficiency (NSE) is 0.77 and 0.80 for calibration and validation period. The monsoonal rain was anticipated to influence stream flow changes the most (46.86%), followed by base flow (37.57%), snow melt (12.17%), and glacier melt (3.18%) form the year 2004-2009 and rain (46.33%), followed by base flow (38.79%), glacier melt (3.27%), and snowmelt (10.77%) from 2011-2020 according to the model. We think the model can perform as an effective tool for research into the dynamics of hydrological systems and prospective effects of climate change on the Himalayan river basins.

Keywords:

Climate change, Degree day factor, Hydrological modelling, Glacio hydrological degree-day model, Tamakoshi River Basin

[a] Department of Applied Science and Chemical Engineering, Pulchowk Campus, IOE, TU, Nepal

[b] Department of Environmental Science and Engineering, Himalayan Cryosphere, Climate and Disaster Research Center (HiCCDRC), School of Science, Kathmandu University, Kavre, Nepal

[c] Department of Applied Sciences and Chemical Engineering, Pulchowk Campus, IOE, TU, Nepal

[a] chaulagainnabin80@gmail.com, [b] rijan@ku.edu.np, [c] khem@ioe.edu.np

IOE Graduate Conference

Certificate of Participation

This certificate is awarded to

Nabin Chaulagain

in recognition of an invaluable contribution as

Paper Presenter

at the 14th IOE Graduate Conference

Organized by Tribhuvan University, IOE, Curriculum and Instructional Material Development Unit (CIMDU) held from November 29 to December 1, 2023 at Pulchowk Campus, Lalitpur, Nepal.

Asst. Prof. Bhim Kumar Dahal, PhD Conference Convener	Assoc. Prof. Indra Prasad Acharya, PhD Campus Chief Pulchowk Campus	Prof. Shashidhar Ram Joshi, PhD Dean Institute of Engineering

Nabin_078MSCCD006.pdf

ORIGINALITY REPORT

19%
SIMILARITY INDEX

PRIMARY SOURCES

1	www.frontiersin.org Internet	232 words — 3%
2	sarahrshannon.github.io Internet	122 words — 2%
3	www.cambridge.org Internet	116 words — 2%
4	link.springer.com Internet	115 words — 2%
5	repository.ju.edu.et Internet	100 words — 1%
6	arxiv.org Internet	77 words — 1%
7	conference.ioe.edu.np Internet	35 words — 1%
8	www.ncbi.nlm.nih.gov Internet	32 words — < 1%
9	Dibesh Khadka, Mukand S. Babel, Sangam Shrestha, Nitin K. Tripathi. "Climate change impact on glacier and snow melt and runoff in Tamakoshi basin	29 words — < 1%